12-14-2020

Two New Finite Element Schemes and Their Analysis for Modeling of Wave Propagation in Graphene

Jichun Li
University of Nevada, Las Vegas, jichun.li@unlv.edu

Results in Applied Mathematics 9 (2021) 100136

Contents lists available at ScienceDirect

Results in Applied Mathematics

journal homepage: www.elsevier.com/locate/results-in-applied-mathematics

Two new finite element schemes and their analysis for modeling of wave propagation in graphene☆

Jichun Li

Department of Mathematical Sciences, University of Nevada, Las Vegas, NV 89154-4020, USA

ARTICLE INFO

Article history:
Received 7 November 2020
Received in revised form 24 November 2020
Accepted 8 December 2020
Available online 14 December 2020

MSC:
78M10
65N30
65F10
78-08

Keywords:
Maxwell's equations
Finite element time-domain methods
Edge elements
Surface plasmon polaritons
Graphene

ABSTRACT

In this paper, we investigate a system of governing equations for modeling wave propagation in graphene. Compared to our previous work (Yang et al., 2020) , here we re-investigate the governing equations by eliminating two auxiliary unknowns from the original model. A totally new stability for the model is established for the first time. Since the finite element scheme proposed in Yang et al. (2020) is only first order in time, here we propose two new schemes with second order convergence in time for the simplified modeling equations. Discrete stabilities inheriting exactly the same form as the continuous stability are proved for both schemes. Convergence error estimates are also established for both schemes. Numerical results are presented to justify our theoretical analysis.

1. Introduction

Graphene is an atom-thick planar sheet of sp^2-bonded carbon atoms packed in a honeycomb lattice. Graphene was first isolated experimentally by Novoselov, Geim and co-workers [1]. Graphene has many amazing properties [2–4], such as extremely high thermal conductivity, high electronic mobility, and low absorption of light over a wide wavelength range, etc. Since its discovery in 2004, the study of graphene has attracted a great interest from researchers in various areas of sciences and engineering, and it has resulted in the 2010 Nobel Prize in Physics to Geim and Novoselov "for groundbreaking experiments regarding the two-dimensional material graphene". (https://www.nobelprize.org/prizes/physics/2010/summary/). Graphene has been exploited in a wide range of applications, including optical devices, photodetectors, metasurfaces, sensors (for sensing mass, gas, tension, charge, diseases, and explosives), low-cost display screens of mobile devices, lithium-ion batteries with fast recharge capacity, and hydrogen storage for fuel cell-powered cars.

Because of the practical difficulties and expenses in physical experiments with graphene, numerical simulation of wave interactions with graphene materials plays a very important role in designing functional components with graphene [4–8]. Due to its computational efficiency and simple implementation, the finite difference time-domain (FDTD) method is arguably the most popular numerical method, especially in the engineering and physics community, and it has been widely used to simulate the electromagnetic wave propagation phenomena in complex media, including metamaterials and

☆ Work supported by National Science Foundation, USA under Grant No. DMS-2011943.
E-mail address: jichun.li@unlv.edu.

https://doi.org/10.1016/j.rinam.2020.100136

graphene (cf. [5–17]). Readers can find more details on the FDTD method and its applications in the monographs [18–20] and the references therein.

Considering our expertise on the finite element method (FEM), we are interested in the finite element time-domain (FETD) method for simulating wave propagation in complex media such as metamaterial and graphene. Thanks to the hard work of researchers, there have been many excellent FEM papers published for solving Maxwell's equations over the past 30 years (e.g., [21–45]). As for FETD, Ciarlet and Zou [46] derived the first optimal convergence order for both interpolation and energy-norm error estimates for time-dependent Maxwell's equations under a practically important regularity $H^{\alpha}(curl)$ with $\frac{1}{2} < \alpha \leq 1$, since the previous interpolation and energy-norm error estimates were obtained for $\alpha \geq 1$. Chen, Du and Zou [47] established optimal error estimates for time-dependent Maxwell equations with discontinuous coefficients in general three-dimensional Lipschitz polyhedral domains solved by finite element methods. Another interesting paper by Ciarlet, Wu and Zou [48] has considered the time-harmonic and time-dependent Maxwell system. And it is also the first time to get the optimal convergence of the divergence law in an most appropriate norm, and previous works do not get the strong convergence of the divergence law, only in the distributional sense. This is very important in many physical applications to keep the entire divergence law reinforced globally. More references can be found in some review papers [49–52] and related books [53–57].

Except some recent works on adaptive FEMs for graphene simulation [58,59], to the best of our knowledge, there exist very few papers on developing and analyzing the FETD methods for simulating graphene materials. Recently, the author and collaborators [60] formulated the time-domain governing equations for simulating the surface plasmon polariton waves in graphene by using the Drude dispersive model for the intraband conductivity and the second order Padé approximation for the interband conductivity. A FETD scheme was proposed and analyzed for solving this model. Extensive numerical results were carried out to simulate the surface plasmon polariton wave propagation. However, the FETD scheme proposed there is only first order in time [60, (3.5)] and involves too many unknowns. Here we carefully investigate the modeling equations of [60] and propose two new second order in time FETD schemes by reducing two auxiliary unknowns from the original model. Totally new stabilities are proved for the continuous model and both FETD schemes. The discrete stabilities inherit the exactly the same form as the stability in the continuous case. Complete convergence analyses are also established for both schemes.

The rest of the paper is organized as follows. In Section 2, we present the time-domain governing equations for modeling the surface plasmon polariton in graphene. Then we prove an energy identity and a stability for the model system. In Section 3, we propose a Crank–Nicolson scheme for the model and prove the discrete stability and error estimate for the scheme. In Section 4, we present a leaf-frog scheme and establish similar discrete stability and error estimate. Then in Section 5 we present numerical results to demonstrate our theoretical analysis. Finally, we conclude the paper in Section 6.

2. The time-domain governing equations

In our recent work [60], we derived the following governing equations for simulating the wave propagation in graphene: for any $(\boldsymbol{x}, t) \in \Omega \times (0, T]$,

$$\epsilon_0 \partial_t \boldsymbol{E} = \nabla \times \boldsymbol{H} - \boldsymbol{J}_d - \boldsymbol{J}_p, \tag{2.1}$$

$$\mu_0 \partial_t \boldsymbol{H} = -\nabla \times \boldsymbol{E}, \tag{2.2}$$

$$\frac{1}{\epsilon_0 \omega_{pe}^2} \partial_t \boldsymbol{J}_d + \frac{\gamma}{\epsilon_0 \omega_{pe}^2} \boldsymbol{J}_d = \boldsymbol{E}, \tag{2.3}$$

$$\partial_{tt} \boldsymbol{J}_p + b_1^* \partial_t \boldsymbol{J}_p + b_2^* \boldsymbol{J}_p = a_2^* \partial_{tt} \boldsymbol{E} + a_1^* \partial_t \boldsymbol{E} + a_0^* \boldsymbol{E}, \tag{2.4}$$

where $\boldsymbol{E}$ and $\boldsymbol{H}$ are the electric and magnetic fields, respectively, ϵ_0 and μ_0 are permittivity and permeability in vacuum, respectively. We assume that Ω is a bounded Lipschitz polyhedral domain in $\mathcal{R}^3$, and T is the final simulation time. Note that (2.4) is obtained by dividing the coefficient b_2 from both sides of (2.6) of [60]. Doing this will eliminate one coefficient parameter and simplify our following analysis. $\boldsymbol{J}_d$ and $\boldsymbol{J}_p$ represent the intraband and interband current density in the graphene layer. The positive constants γ and ω_{pe} are some physical parameters coming from the intraband permittivity. The constants $b_1^*, b_2^*, a_2^*, a_1^*$ and a_0^* are obtained through data matching for the interband conductivity. These numbers can be varied depending on the chemical potential, one group of data is given as [7, Table 1]:

$$a_2 = 1.343e - 36, b_2 = 2.148e - 31, a_1 = 1.674e - 20, b_1 = 8.082e - 17, a_0 = -9.114e - 28, \tag{2.5}$$

which translates to our case as

$$a_2^* = a_2/b_2, \quad a_1^* = a_1/b_2, \quad b_1^* = b_1/b_2, \quad a_0^* = a_0/b_2.$$

Without loss of generality, in the rest of the paper we just assume that $b_1^*, b_2^*, a_2^*, a_1^*$ are positive, and a_0^* is negative. Otherwise, we have to revise the energy (3.40) and analysis accordingly. We want to remark that the system (2.1)–(2.4) models wave propagation in graphene, which is usually embedded inside other materials such as vacuum, see our illustration given in Fig. 1. Furthermore, the system (2.1)–(2.4) can be reduced to the standard Maxwell's equations in vacuum by letting $\boldsymbol{J}_d$ and $\boldsymbol{J}_p$ to be zero, hence we will investigate this more general system directly.

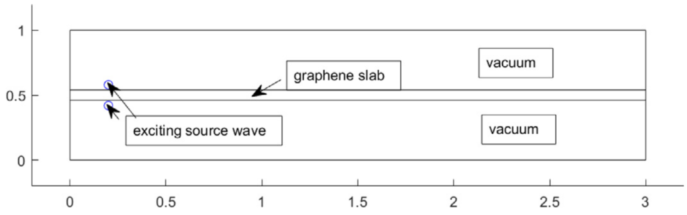

Fig. 1. An illustration of wave propagation in graphene.

To complete the problem, we assume that (2.1)–(2.4) is subject to the perfectly conducting (PEC) boundary condition:

$$\boldsymbol{n} \times \boldsymbol{E} = \boldsymbol{0}, \quad \text{on } \partial\Omega, \tag{2.6}$$

and the initial conditions

$$\boldsymbol{E}(\boldsymbol{x},0) = \boldsymbol{E}_0(\boldsymbol{x}),\ \boldsymbol{H}(\boldsymbol{x},0) = \boldsymbol{H}_0(\boldsymbol{x}),\ \boldsymbol{J}_d(\boldsymbol{x},0) = \boldsymbol{J}_{d0}(\boldsymbol{x}),\ \boldsymbol{J}_p(\boldsymbol{x},0) = \boldsymbol{J}_{p0}(\boldsymbol{x}), \tag{2.7}$$

$$\partial_t \boldsymbol{E}(\boldsymbol{x},0) = \boldsymbol{E}_1(\boldsymbol{x}),\ \partial_t \boldsymbol{J}_p(\boldsymbol{x},0) = \boldsymbol{J}_{p1}(\boldsymbol{x}), \tag{2.8}$$

where $\boldsymbol{n}$ is the unit outward normal vector to $\partial\Omega$, and $\boldsymbol{E}_0, \boldsymbol{H}_0, \boldsymbol{J}_{d0}, \boldsymbol{J}_{p0}, \boldsymbol{E}_1$ and $\boldsymbol{J}_{p1}$ are some given functions.

To simplify the notation, from now on we denote the kth time derivative $\partial_{t^k} u := \frac{\partial^k u}{\partial t^k}$, and $\|u\| := \|u\|_{L^2(\Omega)}$ for the L^2 norm of u in Ω. To prove the stability for the graphene model (2.1)–(2.4), we need to use the following Gronwall inequality.

Lemma 2.1 ([61, p. 624]). *Let $\eta(t)$ be a nonnegative, absolutely continuous function on $[0,T]$, which satisfies the differential inequality*

$$\frac{d}{dt}\eta(t) \le r(t)\eta(t),$$

where $r(t)$ is nonnegative, summable function on $[0,T]$. Then

$$\eta(t) \le \eta(0)\exp(\int_0^t r(s)ds) \quad \forall\, t \in [0,T].$$

Now we can prove the following energy identity and stability for the graphene model (2.1)–(2.4).

Theorem 2.1. *For the solution $(\boldsymbol{E}, \boldsymbol{H}, \boldsymbol{J}_d, \boldsymbol{J}_p)$ of (2.1)–(2.4), the following energy identity holds true for any $t \in [0,T]$:*

$$\begin{aligned} &\frac{1}{2}(ENG(t) - ENG(0)) + \int_0^t \left[\sum_{k=0}^{2} \frac{\gamma}{\epsilon_0 \omega_{pe}^2} \|\partial_{t^k} \boldsymbol{J}_d\|^2 + b_1^* \|\partial_t \boldsymbol{J}_p\|^2 + a_2^* \|\partial_{t^2} \boldsymbol{E}\|^2 \right] dt \\ = &\int_0^t \big[-(\boldsymbol{J}_p, \boldsymbol{E}) + (a_1^* - 1)(\partial_t \boldsymbol{J}_p, \partial_t \boldsymbol{E}) + (a_2^* + b_1^*)(\partial_{t^2} \boldsymbol{E}, \partial_t \boldsymbol{J}_p) \\ &\quad + (b_2^* \boldsymbol{J}_p - a_0^* \boldsymbol{E}, \partial_{t^2} \boldsymbol{E}) + a_0^* (\boldsymbol{E}, \partial_t \boldsymbol{J}_p) \big] dt, \end{aligned} \tag{2.9}$$

where we denote

$$\begin{aligned} ENG(t) = &\Big[\sum_{k=0}^{2} (\epsilon_0 \|\partial_{t^k} \boldsymbol{E}\|^2 + \mu_0 \|\partial_{t^k} \boldsymbol{H}\|^2 + \frac{1}{\epsilon_0 \omega_{pe}^2} \|\partial_{t^k} \boldsymbol{J}_d\|^2) \\ &+ \|\partial_t \boldsymbol{J}_p\|^2 + b_2^* \|\boldsymbol{J}_p\|^2 + a_1^* \|\partial_t \boldsymbol{E}\|^2 \Big](t). \end{aligned} \tag{2.10}$$

Furthermore, we have the following stability:

$$ENG(t) \le ENG(0) \cdot \exp(C_* t), \quad \forall\, t \in [0,T], \tag{2.11}$$

where constant $C_* > 0$ depends on those physical parameters of the model (2.1)–(2.4).

Proof. Multiplying (2.1), (2.2), and (2.3) by $\boldsymbol{E}, \boldsymbol{H}$ and $\boldsymbol{J}_d$, and integrating over Ω respectively, then using the PEC boundary condition (2.6) and summing up the results, we have

$$\frac{1}{2}\frac{d}{dt}(\epsilon_0 \|\boldsymbol{E}\|^2 + \mu_0 \|\boldsymbol{H}\|^2 + \frac{1}{\epsilon_0 \omega_{pe}^2} \|\boldsymbol{J}_d\|^2) + \frac{\gamma}{\epsilon_0 \omega_{pe}^2} \|\boldsymbol{J}_d\|^2 = -(\boldsymbol{J}_p, \boldsymbol{E}). \tag{2.12}$$

Similarly, using the linearity, we can first take the kth time derivative of (2.1), (2.2), and (2.3), then multiply the resulting equations by $\partial_{t^k}\boldsymbol{E}$, $\partial_{t^k}\boldsymbol{H}$, $\partial_{t^k}\boldsymbol{J}_d$, and integrate over Ω, respectively, to obtain: For any $k \geq 1$,

$$\frac{1}{2}\frac{d}{dt}(\epsilon_0\|\partial_{t^k}\boldsymbol{E}\|^2 + \mu_0\|\partial_{t^k}\boldsymbol{H}\|^2 + \frac{1}{\epsilon_0\omega_{pe}^2}\|\partial_{t^k}\boldsymbol{J}_d\|^2) + \frac{\gamma}{\epsilon_0\omega_{pe}^2}\|\partial_{t^k}\boldsymbol{J}_d\|^2 = -(\partial_{t^k}\boldsymbol{J}_p, \partial_{t^k}\boldsymbol{E}). \tag{2.13}$$

If we treat $\partial_t^0 = I$ (the identity operator), then (2.12) is just a special case of (2.13) with $k = 0$.

Multiplying (2.4) by $\partial_t\boldsymbol{J}_p$, and integrating over Ω, we have

$$\begin{aligned}&\frac{1}{2}\frac{d}{dt}(\|\partial_t\boldsymbol{J}_p\|^2 + b_2^*\|\boldsymbol{J}_p\|^2) + b_1^*\|\partial_t\boldsymbol{J}_p\|^2\\ &= (a_2^*\partial_{t^2}\boldsymbol{E} + a_1^*\partial_t\boldsymbol{E} + a_0^*\boldsymbol{E}, \partial_t\boldsymbol{J}_p).\end{aligned} \tag{2.14}$$

Adding up (2.12), (2.13) with $k = 1, 2$, and (2.14), we obtain

$$\begin{aligned}&\frac{1}{2}\frac{d}{dt}\left[\sum_{k=0}^{2}(\epsilon_0\|\partial_{t^k}\boldsymbol{E}\|^2 + \mu_0\|\partial_{t^k}\boldsymbol{H}\|^2 + \frac{1}{\epsilon_0\omega_{pe}^2}\|\partial_{t^k}\boldsymbol{J}_d\|^2) + \|\partial_t\boldsymbol{J}_p\|^2 + b_2^*\|\boldsymbol{J}_p\|^2\right]\\ &\qquad + \sum_{k=0}^{2}\frac{\gamma}{\epsilon_0\omega_{pe}^2}\|\partial_{t^k}\boldsymbol{J}_d\|^2 + b_1^*\|\partial_t\boldsymbol{J}_p\|^2\\ &= -\sum_{k=0}^{2}(\partial_{t^k}\boldsymbol{J}_p, \partial_{t^k}\boldsymbol{E}) + (a_2^*\partial_{t^2}\boldsymbol{E} + a_1^*\partial_t\boldsymbol{E} + a_0^*\boldsymbol{E}, \partial_t\boldsymbol{J}_p).\end{aligned} \tag{2.15}$$

Using (2.4), we further have

$$\begin{aligned}&(\partial_{t^2}\boldsymbol{J}_p, \partial_{t^2}\boldsymbol{E}) = (a_2^*\partial_{t^2}\boldsymbol{E} + a_1^*\partial_t\boldsymbol{E} + a_0^*\boldsymbol{E} - b_1^*\partial_t\boldsymbol{J}_p - b_2^*\boldsymbol{J}_p, \partial_{t^2}\boldsymbol{E})\\ &= a_2^*\|\partial_{t^2}\boldsymbol{E}\|^2 + \frac{a_1^*}{2}\frac{d}{dt}\|\partial_t\boldsymbol{E}\|^2 + (a_0^*\boldsymbol{E} - b_1^*\partial_t\boldsymbol{J}_p - b_2^*\boldsymbol{J}_p, \partial_{t^2}\boldsymbol{E}).\end{aligned} \tag{2.16}$$

Substituting (2.16) into (2.15) and combining like terms, we have

$$\begin{aligned}&\frac{1}{2}\frac{d}{dt}\left[\sum_{k=0}^{2}(\epsilon_0\|\partial_{t^k}\boldsymbol{E}\|^2 + \mu_0\|\partial_{t^k}\boldsymbol{H}\|^2 + \frac{1}{\epsilon_0\omega_{pe}^2}\|\partial_{t^k}\boldsymbol{J}_d\|^2) + \|\partial_t\boldsymbol{J}_p\|^2 + b_2^*\|\boldsymbol{J}_p\|^2 + a_1^*\|\partial_t\boldsymbol{E}\|^2\right]\\ &\qquad + \sum_{k=0}^{2}\frac{\gamma}{\epsilon_0\omega_{pe}^2}\|\partial_{t^k}\boldsymbol{J}_d\|^2 + b_1^*\|\partial_t\boldsymbol{J}_p\|^2 + a_2^*\|\partial_{t^2}\boldsymbol{E}\|^2 \\ &= -(\boldsymbol{J}_p, \boldsymbol{E}) + (a_1^* - 1)(\partial_t\boldsymbol{J}_p, \partial_t\boldsymbol{E}) + (a_2^* + b_1^*)(\partial_{t^2}\boldsymbol{E}, \partial_t\boldsymbol{J}_p) + (b_2^*\boldsymbol{J}_p - a_0^*\boldsymbol{E}, \partial_{t^2}\boldsymbol{E}) + a_0^*(\boldsymbol{E}, \partial_t\boldsymbol{J}_p).\end{aligned} \tag{2.17}$$

Integrating (2.17) with respect to time from 0 to t and using the energy notation defined in Theorem 2.1, we complete the proof of the energy identity (2.9).

To prove the stability (2.11), by dropping the last nonnegative terms on the left hand side (LHS) of (2.17), we have

$$\begin{aligned}&\frac{1}{2}\frac{d}{dt}\left[\sum_{k=0}^{2}(\epsilon_0\|\partial_{t^k}\boldsymbol{E}\|^2 + \mu_0\|\partial_{t^k}\boldsymbol{H}\|^2 + \frac{1}{\epsilon_0\omega_{pe}^2}\|\partial_{t^k}\boldsymbol{J}_d\|^2) + \|\partial_t\boldsymbol{J}_p\|^2 + b_2^*\|\boldsymbol{J}_p\|^2 + a_1^*\|\partial_t\boldsymbol{E}\|^2\right]\\ &\leq -(\boldsymbol{J}_p, \boldsymbol{E}) + (a_1^* - 1)(\partial_t\boldsymbol{J}_p, \partial_t\boldsymbol{E}) + (a_2^* + b_1^*)(\partial_{t^2}\boldsymbol{E}, \partial_t\boldsymbol{J}_p)\\ &\qquad + (b_2^*\boldsymbol{J}_p - a_0^*\boldsymbol{E}, \partial_{t^2}\boldsymbol{E}) + a_0^*(\boldsymbol{E}, \partial_t\boldsymbol{J}_p).\end{aligned} \tag{2.18}$$

Note that all the right hand side (RHS) terms of (2.18) can be bounded by the corresponding terms on the LHS. For example, using the inequality $ab \leq \frac{1}{2}(a^2 + b^2)$, we have

$$(\boldsymbol{J}_p, \boldsymbol{E}) = \frac{1}{\sqrt{\epsilon_0 b_2^*}}(\sqrt{b_2^*}\boldsymbol{J}_p, \sqrt{\epsilon_0}\boldsymbol{E}) \leq \frac{1}{2\sqrt{\epsilon_0 b_2^*}}(b_2^*\|\boldsymbol{J}_p\|^2 + \epsilon_0\|\boldsymbol{E}\|^2).$$

Applying all these estimates for the RHS terms of (2.18) and the Gronwall inequality given by Lemma 2.1, we easily complete the proof of (2.11). □

3. The Crank–Nicolson scheme and its analysis

To develop a time discretization scheme, we divide the time interval $I = [0, T]$ into N uniform subintervals $I_i = [t_{i-1}, t_i]$ by points $t_n = n\tau, n = 0, 1, \ldots, N$, where $\tau = \frac{T}{N}$. Furthermore, we introduce the following central difference operators in time: For any time sequence function u^n,

$$\delta_\tau u^{n+\frac{1}{2}} = \frac{u^{n+1} - u^n}{\tau}, \quad \delta_{2\tau} u^n = \frac{u^{n+1} - u^{n-1}}{2\tau},$$

and averaging operators:

$$\overline{u}^{n+\frac{1}{2}} = \frac{u^{n+1}+u^n}{2}, \quad \widetilde{u}^n = \frac{u^{n+1}+u^{n-1}}{2}.$$

To design our finite element method, we partition Ω by a family of regular elements $\mathcal{T}_h$ with maximum mesh size h. Without loss of generality, we consider the following Raviart–Thomas–Nédélec's mixed spaces U_h and V_h on tetrahedral elements. On any tetrahedral element $e \in \mathcal{T}_h$ and any $p \geq 1$, we choose [55]

$$U_h = \{\psi_h \in H(div;\Omega): \ \psi_h|_e \in D_p, \ \forall e \in \mathcal{T}_h\},$$
$$\boldsymbol{V}_h = \{\phi_h \in H(curl;\Omega): \ \phi_h|_e \in R_p, \ \forall e \in \mathcal{T}_h\},$$

where $D_p = (P_{p-1})^3 \oplus \boldsymbol{x}\tilde{P}_{p-1}$ and $R_p = (P_{p-1})^3 \oplus \mathcal{S}_p$ are vector polynomial spaces. Moreover, P_{p-1} represents a polynomial of maximum total degree $p-1$, $\tilde{P}_{p-1}$ denotes a homogeneous polynomial of degree $p-1$, and $\mathcal{S}_p := \left\{\mathbf{p} \in (\tilde{P}_p)^3 \mid \boldsymbol{x}\cdot\mathbf{p} = 0\right\}$ denotes a subspace of homogeneous vector polynomials of degree p. To impose the perfect conducting boundary condition $\boldsymbol{n}\times\boldsymbol{E} = 0$, we introduce the space

$$\boldsymbol{V}_h^0 = \{\phi_h \in \boldsymbol{V}_h: \quad \boldsymbol{n}\times\phi_h = 0 \quad \text{on } \partial\Omega\}.$$

Using the Crank–Nicolson time discretization method, we can develop the following Crank–Nicolson (CN) scheme for solving (2.1)–(2.4): Given proper initial approximations $(\boldsymbol{E}_h^0, \boldsymbol{J}_{d,h}^0, \boldsymbol{J}_{p,h}^0, \boldsymbol{H}_h^0, \boldsymbol{E}_h^{-1}, \boldsymbol{J}_{p,h}^{-1})$, for any $n \geq 0$, solve for $(\boldsymbol{E}_h^{n+1}, \boldsymbol{J}_{d,h}^{n+1}, \boldsymbol{J}_{p,h}^{n+1}, \boldsymbol{H}_h^{n+1}) \in (\boldsymbol{V}_h^0)^3 \times U_h$ satisfying the following:

$$\epsilon_0(\delta_\tau \boldsymbol{E}_h^{n+\frac{1}{2}}, \phi_h) = (\overline{\boldsymbol{H}}_h^{n+\frac{1}{2}}, \nabla\times\phi_h) - (\overline{\boldsymbol{J}}_{d,h}^{n+\frac{1}{2}}, \phi_h) - (\overline{\boldsymbol{J}}_{p,h}^{n+\frac{1}{2}}, \phi_h), \tag{3.19}$$

$$\mu_0(\delta_\tau \boldsymbol{H}_h^{n+\frac{1}{2}}, \psi_h) = -(\nabla\times\overline{\boldsymbol{E}}_h^{n+\frac{1}{2}}, \psi_h), \tag{3.20}$$

$$\left(\frac{1}{\epsilon_0\omega_{pe}^2}\delta_\tau \boldsymbol{J}_{d,h}^{n+\frac{1}{2}} + \frac{\gamma}{\epsilon_0\omega_{pe}^2}\overline{\boldsymbol{J}}_{d,h}^{n+\frac{1}{2}}, \phi_h\right) = (\overline{\boldsymbol{E}}_h^{n+\frac{1}{2}}, \phi_h) \tag{3.21}$$

$$(\delta_\tau^2 \boldsymbol{J}_{p,h}^n + b_1^*\delta_{2\tau}\boldsymbol{J}_{p,h}^n + b_2^*\widetilde{\boldsymbol{J}}_{p,h}^n, \phi_h) = (a_2^*\delta_\tau^2\boldsymbol{E}_h^n + a_1^*\delta_{2\tau}\boldsymbol{E}_h^n + a_0^*\boldsymbol{E}_h^n, \phi_h), \tag{3.22}$$

for any $\phi_h \in \boldsymbol{V}_h^0$ and $\psi_h \in U_h$. Moreover we used the second order central difference operator defined as:

$$\delta_\tau^2 u^n := \delta_\tau(\delta_\tau u^n) = \frac{\delta_\tau u^{n+\frac{1}{2}} - \delta_\tau u^{n-\frac{1}{2}}}{\tau} = \frac{u^{n+1}-2u^n+u^{n-1}}{\tau^2}.$$

We like to remark that replacing the last term $\boldsymbol{E}_h^n$ in (3.22) by $\widetilde{\boldsymbol{E}}_h^n$ creates a challenge in proving the stability of this scheme after we tried. The initial conditions (2.7)–(2.8) are discretized as follows:

$$\boldsymbol{E}_h^0 = \Pi_c\boldsymbol{E}_0(\boldsymbol{x}), \ \boldsymbol{H}_h^0 = \Pi_2\boldsymbol{H}_0(\boldsymbol{x}), \ \boldsymbol{J}_{d,h}^0 = \Pi_c\boldsymbol{J}_{d0}(\boldsymbol{x}), \ \boldsymbol{J}_{p,h}^0 = \Pi_c\boldsymbol{J}_{p0}(\boldsymbol{x}), \tag{3.23}$$

$$\delta_{2\tau}\boldsymbol{E}_h^0 := \frac{\boldsymbol{E}_h^1 - \boldsymbol{E}_h^{-1}}{2\tau} = \Pi_c\boldsymbol{E}_1(\boldsymbol{x}), \quad \delta_{2\tau}\boldsymbol{J}_{p,h}^0 := \frac{\boldsymbol{J}_{p,h}^1 - \boldsymbol{J}_{p,h}^{-1}}{2\tau} = \Pi_c\boldsymbol{J}_{p1}(\boldsymbol{x}), \tag{3.24}$$

where Π_c is the Nédélec interpolation in space $\boldsymbol{V}_h$, and Π_2 is the standard L^2 projection into space U_h.

Denote the modulo operator $[k] := k \bmod 2$, i.e., $[k] = 0$ when k is even, and $[k] = 1$ when k is odd. For the Crank–Nicolson scheme (3.19)–(3.22), we have the following discrete form of the continuous energy identity (2.17) obtained in Theorem 2.1.

Theorem 3.1.

$$\begin{aligned}
&\frac{1}{2}\delta_\tau\left[\sum_{k=0}^{2}\left(\epsilon_0\|\delta_\tau^k\boldsymbol{E}_h^{n+\frac{[k+1]}{2}}\|^2 + \mu_0\|\delta_\tau^k\boldsymbol{H}_h^{n+\frac{[k+1]}{2}}\|^2 + \frac{1}{\epsilon_0\omega_{pe}^2}\|\delta_\tau^k\boldsymbol{J}_{d,h}^{n+\frac{[k+1]}{2}}\|^2\right) + \|\delta_\tau\boldsymbol{J}_{p,h}^{n+1}\|^2\right.\\
&\left.+a_1^*\|\delta_\tau\overline{\boldsymbol{E}}_h^{n+\frac{1}{2}}\|^2\right] + \frac{b_2^*}{2}\delta_{2\tau}\|\boldsymbol{J}_{p,h}^{n+1}\|^2 + \sum_{k=0}^{2}\frac{\gamma}{\epsilon_0\omega_{pe}^2}\|\delta_\tau^k\overline{\boldsymbol{J}}_{d,h}^{n+\frac{[k+1]}{2}}\|^2 + b_1^*\|\delta_\tau\overline{\boldsymbol{J}}_{p,h}^{n+1}\|^2 + a_2^*\|\delta_\tau^2\overline{\boldsymbol{E}}_h^{n+\frac{1}{2}}\|^2\\
&\qquad = -(\overline{\boldsymbol{J}}_{p,h}^{n+\frac{1}{2}}, \overline{\boldsymbol{E}}_h^{n+\frac{1}{2}}) - (\delta_\tau\overline{\boldsymbol{J}}_{p,h}^{n}, \delta_\tau\overline{\boldsymbol{E}}_h^{n}) + a_1^*(\delta_\tau\overline{\boldsymbol{J}}_{p,h}^{n+1}, \delta_\tau\overline{\boldsymbol{E}}_h^{n+1})\\
&\qquad\quad + \left(\frac{b_1^*}{2}(\delta_\tau\overline{\boldsymbol{J}}_{p,h}^{n+1} + \delta_\tau\overline{\boldsymbol{J}}_{p,h}^{n}) + b_2^*\overline{\widetilde{\boldsymbol{J}}_{p,h}}^{n+\frac{1}{2}} - a_0^*\overline{\boldsymbol{E}}_h^{n+\frac{1}{2}}, \delta_\tau^2\overline{\boldsymbol{E}}_h^{n+\frac{1}{2}}\right)\\
&\qquad\qquad + (a_2^*\delta_\tau^2\boldsymbol{E}_h^{n+1} + a_0^*\boldsymbol{E}_h^{n+1}, \delta_\tau\overline{\boldsymbol{J}}_{p,h}^{n+1}).
\end{aligned} \tag{3.25}$$

Proof. Since the proof is lengthy and technical, we break the proof into several major steps to make it easy to follow.

(I) Choosing $\phi_h = \overline{\boldsymbol{E}}_h^{n+\frac{1}{2}}$, $\psi_h = \overline{\boldsymbol{H}}_h^{n+\frac{1}{2}}$, and $\phi_h = \overline{\boldsymbol{J}}_{d,h}^{n+\frac{1}{2}}$ in (3.19), (3.20), and (3.21), respectively, then summing up the results, we have

$$\begin{aligned} &\frac{1}{2}\delta_\tau\left[\epsilon_0\|\boldsymbol{E}_h^{n+\frac{1}{2}}\|^2 + \mu_0\|\boldsymbol{H}_h^{n+\frac{1}{2}}\|^2 + \frac{1}{\epsilon_0\omega_{pe}^2}\|\boldsymbol{J}_{d,h}^{n+\frac{1}{2}}\|^2\right] + \frac{\gamma}{\epsilon_0\omega_{pe}^2}\|\overline{\boldsymbol{J}}_{d,h}^{n+\frac{1}{2}}\|^2 \\ &= -(\overline{\boldsymbol{J}}_{p,h}^{n+\frac{1}{2}}, \overline{\boldsymbol{E}}_h^{n+\frac{1}{2}}). \end{aligned} \tag{3.26}$$

(II) Using (3.19)–(3.21) to subtract themselves with n reduced by $n-1$, then dividing the results by τ, we obtain

$$\epsilon_0(\delta_\tau^2\boldsymbol{E}_h^n, \phi_h) = (\delta_\tau\overline{\boldsymbol{H}}_h^n, \nabla\times\phi_h) - (\delta_\tau\overline{\boldsymbol{J}}_{d,h}^n, \phi_h) - (\delta_\tau\overline{\boldsymbol{J}}_{p,h}^n, \phi_h), \tag{3.27}$$

$$\mu_0(\delta_\tau^2\boldsymbol{H}_h^n, \psi_h) = -(\nabla\times\delta_\tau\overline{\boldsymbol{E}}_h^n, \psi_h), \tag{3.28}$$

$$(\frac{1}{\epsilon_0\omega_{pe}^2}\delta_\tau^2\boldsymbol{J}_{d,h}^n + \frac{\gamma}{\epsilon_0\omega_{pe}^2}\delta_\tau\overline{\boldsymbol{J}}_{d,h}^n, \phi_h) = (\delta_\tau\overline{\boldsymbol{E}}_h^n, \phi_h). \tag{3.29}$$

Choosing $\phi_h = \delta_\tau\overline{\boldsymbol{E}}_h^n$, $\psi_h = \delta_\tau\overline{\boldsymbol{H}}_h^n$, and $\phi_h = \delta_\tau\overline{\boldsymbol{J}}_{d,h}^n$ in (3.27), (3.28), and (3.29), respectively, and summing up the results, we have

$$\begin{aligned} &\frac{1}{2}\delta_\tau\left[\epsilon_0\|\delta_\tau\boldsymbol{E}_h^n\|^2 + \mu_0\|\delta_\tau\boldsymbol{H}_h^n\|^2 + \frac{1}{\epsilon_0\omega_{pe}^2}\|\delta_\tau\boldsymbol{H}_h^n\|^2\right] + \frac{\gamma}{\epsilon_0\omega_{pe}^2}\|\delta_\tau\overline{\boldsymbol{J}}_{d,h}^n\|^2 \\ &= -(\delta_\tau\overline{\boldsymbol{J}}_{p,h}^n, \delta_\tau\overline{\boldsymbol{E}}_h^n). \end{aligned} \tag{3.30}$$

(III) Using the third order central difference operator

$$\delta_\tau^3 u^{n+\frac{1}{2}} = \delta_\tau(\delta_\tau^2 u^{n+\frac{1}{2}}) = \frac{\delta_\tau^2 u^{n+1} - \delta_\tau^2 u^n}{\tau},$$

and subtracting (3.27)–(3.29) from themselves with n replaced by $n+1$, we obtain

$$\epsilon_0(\delta_\tau^3\boldsymbol{E}_h^{n+\frac{1}{2}}, \phi_h) = (\delta_\tau^2\overline{\boldsymbol{H}}_h^{n+\frac{1}{2}}, \nabla\times\phi_h) - (\delta_\tau^2\overline{\boldsymbol{J}}_{d,h}^{n+\frac{1}{2}}, \phi_h) - (\delta_\tau^2\overline{\boldsymbol{J}}_{p,h}^{n+\frac{1}{2}}, \phi_h), \tag{3.31}$$

$$\mu_0(\delta_\tau^3\boldsymbol{H}_h^{n+\frac{1}{2}}, \psi_h) = -(\nabla\times\delta_\tau^2\overline{\boldsymbol{E}}_h^{n+\frac{1}{2}}, \psi_h), \tag{3.32}$$

$$(\frac{1}{\epsilon_0\omega_{pe}^2}\delta_\tau^3\boldsymbol{J}_{d,h}^{n+\frac{1}{2}} + \frac{\gamma}{\epsilon_0\omega_{pe}^2}\delta_\tau^2\overline{\boldsymbol{J}}_{d,h}^{n+\frac{1}{2}}, \phi_h) = (\delta_\tau^2\overline{\boldsymbol{E}}_h^{n+\frac{1}{2}}, \phi_h). \tag{3.33}$$

Choosing $\phi_h = \delta_\tau^2\overline{\boldsymbol{E}}_h^{n+\frac{1}{2}}$, $\delta_\tau^2\overline{\boldsymbol{H}}_h^{n+\frac{1}{2}}$, and $\delta_\tau^2\overline{\boldsymbol{J}}_{d,h}^{n+\frac{1}{2}}$ in (3.31), (3.32), and (3.33), respectively, then adding up the results, we have

$$\begin{aligned} &\frac{1}{2}\delta_\tau\left[\epsilon_0\|\delta_\tau^2\boldsymbol{E}_h^{n+\frac{1}{2}}\|^2 + \mu_0\|\delta_\tau^2\boldsymbol{H}_h^{n+\frac{1}{2}}\|^2 + \frac{1}{\epsilon_0\omega_{pe}^2}\|\delta_\tau^2\boldsymbol{J}_{d,h}^{n+\frac{1}{2}}\|^2\right] + \frac{\gamma}{\epsilon_0\omega_{pe}^2}\|\delta_\tau^2\overline{\boldsymbol{J}}_{d,h}^{n+\frac{1}{2}}\|^2 \\ &= -(\delta_\tau^2\overline{\boldsymbol{J}}_{p,h}^{n+\frac{1}{2}}, \delta_\tau^2\overline{\boldsymbol{E}}_h^{n+\frac{1}{2}}). \end{aligned} \tag{3.34}$$

(IV) Choosing $\phi_h = \delta_\tau\overline{\boldsymbol{J}}_{p,h}^n$ in (3.22), then using the following identities

$$\begin{aligned} &(\delta_\tau^2\boldsymbol{J}_{p,h}^n, \delta_\tau\overline{\boldsymbol{J}}_{p,h}^n) = \left(\frac{\delta_\tau\boldsymbol{J}_{p,h}^{n+\frac{1}{2}} - \delta_\tau\boldsymbol{J}_{p,h}^{n-\frac{1}{2}}}{\tau}, \delta_\tau(\frac{\boldsymbol{J}_{p,h}^{n+\frac{1}{2}} + \boldsymbol{J}_{p,h}^{n-\frac{1}{2}}}{2})\right) \\ &= \frac{1}{2\tau}(\|\delta_\tau\boldsymbol{J}_{p,h}^{n+\frac{1}{2}}\|^2 - \|\delta_\tau\boldsymbol{J}_{p,h}^{n-\frac{1}{2}}\|^2) = \frac{1}{2}\delta_\tau\|\delta_\tau\boldsymbol{J}_{p,h}^n\|^2, \\ &(\delta_{2\tau}\boldsymbol{J}_{p,h}^n, \delta_\tau\overline{\boldsymbol{J}}_{p,h}^n) = \left(\frac{(\boldsymbol{J}_{p,h}^{n+1} - \boldsymbol{J}_{p,h}^n) + (\boldsymbol{J}_{p,h}^n - \boldsymbol{J}_{p,h}^{n-1})}{2\tau}, \delta_\tau(\frac{\boldsymbol{J}_{p,h}^{n+\frac{1}{2}} + \boldsymbol{J}_{p,h}^{n-\frac{1}{2}}}{2})\right) \\ &\qquad = \left(\frac{\delta_\tau\boldsymbol{J}_{p,h}^{n+\frac{1}{2}} + \delta_\tau\boldsymbol{J}_{p,h}^{n-\frac{1}{2}}}{2}, \delta_\tau(\frac{\boldsymbol{J}_{p,h}^{n+\frac{1}{2}} + \boldsymbol{J}_{p,h}^{n-\frac{1}{2}}}{2})\right) = \|\delta_\tau\overline{\boldsymbol{J}}_{p,h}^n\|^2, \end{aligned}$$

and

$$\begin{aligned} &(\widetilde{\boldsymbol{J}}_{p,h}^n, \delta_\tau\overline{\boldsymbol{J}}_{p,h}^n) = (\frac{\boldsymbol{J}_{p,h}^{n+1} + \boldsymbol{J}_{p,h}^{n-1}}{2}, \frac{\overline{\boldsymbol{J}}_{p,h}^{n+\frac{1}{2}} - \overline{\boldsymbol{J}}_{p,h}^{n-\frac{1}{2}}}{\tau}) \\ &= (\frac{\boldsymbol{J}_{p,h}^{n+1} + \boldsymbol{J}_{p,h}^{n-1}}{2}, \frac{(\boldsymbol{J}_{p,h}^{n+1} + \boldsymbol{J}_{p,h}^n) - (\boldsymbol{J}_{p,h}^n + \boldsymbol{J}_{p,h}^{n-1})}{2\tau}) = \frac{\|\boldsymbol{J}_{p,h}^{n+1}\|^2 - \|\boldsymbol{J}_{p,h}^{n-1}\|^2}{4\tau} = \frac{1}{2}\delta_{2\tau}\|\boldsymbol{J}_{p,h}^n\|^2, \end{aligned}$$

we obtain

$$\frac{1}{2}\delta_\tau\|\delta_\tau \boldsymbol{J}^n_{p,h}\|^2 + b_1^*\|\delta_\tau \overline{\boldsymbol{J}}^n_{p,h}\|^2 + \frac{b_2^*}{2}\delta_{2\tau}\|\boldsymbol{J}^n_{p,h}\|^2$$
$$= (a_2^*\delta_\tau^2\boldsymbol{E}^n + a_1^*\delta_{2\tau}\boldsymbol{E}^n + a_0^*\boldsymbol{E}^n, \delta_\tau\overline{\boldsymbol{J}}^n_{p,h}). \tag{3.35}$$

(V) Adding up (3.26), (3.30), (3.34), and (3.35) with n replaced by $n+1$, and using the previously defined modular operator $[k]$ and the short notation $\delta_\tau^0 = I$, we have

$$\frac{1}{2}\delta_\tau\left[\sum_{k=0}^{2}(\epsilon_0\|\delta_\tau^k\boldsymbol{E}_h^{n+\frac{[k+1]}{2}}\|^2 + \mu_0\|\delta_\tau^k\boldsymbol{H}_h^{n+\frac{[k+1]}{2}}\|^2 + \frac{1}{\epsilon_0\omega_{pe}^2}\|\delta_\tau^k\boldsymbol{J}_{d,h}^{n+\frac{[k+1]}{2}}\|^2) + \|\delta_\tau\boldsymbol{J}^{n+1}_{p,h}\|^2\right]$$
$$+\frac{b_2^*}{2}\delta_{2\tau}\|\boldsymbol{J}^{n+1}_{p,h}\|^2 + \sum_{k=0}^{2}\frac{\gamma}{\epsilon_0\omega_{pe}^2}\|\delta_\tau^k\overline{\boldsymbol{J}}_{d,h}^{n+\frac{[k+1]}{2}}\|^2 + b_1^*\|\delta_\tau\overline{\boldsymbol{J}}^{n+1}_{p,h}\|^2$$
$$= -(\overline{\boldsymbol{J}}^{n+\frac{1}{2}}_{p,h}, \overline{\boldsymbol{E}}_h^{n+\frac{1}{2}}) - (\delta_\tau\overline{\boldsymbol{J}}^n_{p,h}, \delta_\tau\overline{\boldsymbol{E}}^n_h) - (\delta_\tau^2\overline{\boldsymbol{J}}^{n+\frac{1}{2}}_{p,h}, \delta_\tau^2\overline{\boldsymbol{E}}_h^{n+\frac{1}{2}})$$
$$+(a_2^*\delta_\tau^2\boldsymbol{E}_h^{n+1} + a_1^*\delta_{2\tau}\boldsymbol{E}_h^{n+1} + a_0^*\boldsymbol{E}_h^{n+1}, \delta_\tau\overline{\boldsymbol{J}}^{n+1}_{p,h}). \tag{3.36}$$

(VI) To make our discrete energy identity (3.36) look more similar to the continuous case proved in Theorem 2.1, by using (3.22) with $\phi_h = \delta_\tau^2\overline{\boldsymbol{E}}_h^{n+\frac{1}{2}}$ we can simplify the third term on the RHS of (3.36) to the following:

$$(\delta_\tau^2\overline{\boldsymbol{J}}^{n+\frac{1}{2}}_{p,h}, \delta_\tau^2\overline{\boldsymbol{E}}_h^{n+\frac{1}{2}}) = (\delta_\tau^2(\frac{\boldsymbol{J}^{n+1}_{p,h}+\boldsymbol{J}^n_{p,h}}{2}), \delta_\tau^2\overline{\boldsymbol{E}}_h^{n+\frac{1}{2}})$$
$$= (a_2^*\delta_\tau^2\overline{\boldsymbol{E}}_h^{n+\frac{1}{2}} + a_1^*\delta_{2\tau}\overline{\boldsymbol{E}}_h^{n+\frac{1}{2}} + a_0^*\overline{\boldsymbol{E}}_h^{n+\frac{1}{2}} - b_1^*\delta_{2\tau}\overline{\boldsymbol{J}}^{n+\frac{1}{2}}_{p,h} - b_2^*\overline{\overline{\boldsymbol{J}}}^{n+\frac{1}{2}}_{p,h}, \delta_\tau^2\overline{\boldsymbol{E}}_h^{n+\frac{1}{2}}) \tag{3.37}$$
$$= a_2^*\|\delta_\tau^2\overline{\boldsymbol{E}}_h^{n+\frac{1}{2}}\|^2 + \frac{a_1^*}{2}\delta_\tau\|\delta_\tau\overline{\boldsymbol{E}}_h^{n+\frac{1}{2}}\|^2 + (a_0^*\overline{\boldsymbol{E}}_h^{n+\frac{1}{2}} - b_1^*\delta_{2\tau}\overline{\boldsymbol{J}}^{n+\frac{1}{2}}_{p,h} - b_2^*\overline{\overline{\boldsymbol{J}}}^{n+\frac{1}{2}}_{p,h}, \delta_\tau^2\overline{\boldsymbol{E}}_h^{n+\frac{1}{2}}),$$

where we used the following identity

$$(\delta_{2\tau}\overline{\boldsymbol{E}}_h^{n+\frac{1}{2}}, \delta_\tau^2\overline{\boldsymbol{E}}_h^{n+\frac{1}{2}}) = (\frac{\overline{\boldsymbol{E}}_h^{n+\frac{3}{2}} - \overline{\boldsymbol{E}}_h^{n-\frac{1}{2}}}{2\tau}, \frac{\delta_\tau\overline{\boldsymbol{E}}_h^{n+1} - \delta_\tau\overline{\boldsymbol{E}}_h^n}{\tau})$$
$$= (\frac{(\overline{\boldsymbol{E}}_h^{n+\frac{3}{2}} - \overline{\boldsymbol{E}}_h^{n+\frac{1}{2}}) + (\overline{\boldsymbol{E}}_h^{n+\frac{1}{2}} - \overline{\boldsymbol{E}}_h^{n-\frac{1}{2}})}{2\tau}, \frac{\delta_\tau\overline{\boldsymbol{E}}_h^{n+1} - \delta_\tau\overline{\boldsymbol{E}}_h^n}{\tau}) \tag{3.38}$$
$$= (\frac{\delta_\tau\overline{\boldsymbol{E}}_h^{n+1} + \delta_\tau\overline{\boldsymbol{E}}_h^n}{2}, \frac{\delta_\tau\overline{\boldsymbol{E}}_h^{n+1} - \delta_\tau\overline{\boldsymbol{E}}_h^n}{\tau}) = \frac{1}{2\tau}(\|\delta_\tau\overline{\boldsymbol{E}}_h^{n+1}\|^2 - \|\delta_\tau\overline{\boldsymbol{E}}_h^n\|^2) = \frac{1}{2}\delta_\tau\|\delta_\tau\overline{\boldsymbol{E}}_h^{n+\frac{1}{2}}\|^2.$$

Substituting (3.37) into (3.36) and using the identities

$$\delta_{2\tau}\boldsymbol{E}_h^{n+1} = \frac{(\boldsymbol{E}_h^{n+2} - \boldsymbol{E}_h^{n+1}) + (\boldsymbol{E}_h^{n+1} - \boldsymbol{E}_h^n)}{2\tau} = \frac{\delta_\tau\boldsymbol{E}_h^{n+\frac{3}{2}} + \delta_\tau\boldsymbol{E}_h^{n+\frac{1}{2}}}{2} = \delta_\tau\overline{\boldsymbol{E}}_h^{n+1},$$

and

$$\delta_{2\tau}\overline{\boldsymbol{J}}^{n+\frac{1}{2}}_{p,h} = \frac{\overline{\boldsymbol{J}}^{n+\frac{3}{2}}_{p,h} - \overline{\boldsymbol{J}}^{n-\frac{1}{2}}_{p,h}}{2\tau} = \frac{\delta_\tau\overline{\boldsymbol{J}}^{n+1}_{p,h} + \delta_\tau\overline{\boldsymbol{J}}^n_{p,h}}{2},$$

we can further simplify (3.36) to

$$\frac{1}{2}\delta_\tau\left[\sum_{k=0}^{2}(\epsilon_0\|\delta_\tau^k\boldsymbol{E}_h^{n+\frac{[k+1]}{2}}\|^2 + \mu_0\|\delta_\tau^k\boldsymbol{H}_h^{n+\frac{[k+1]}{2}}\|^2 + \frac{1}{\epsilon_0\omega_{pe}^2}\|\delta_\tau^k\boldsymbol{J}_{d,h}^{n+\frac{[k+1]}{2}}\|^2) + \|\delta_\tau\boldsymbol{J}^{n+1}_{p,h}\|^2\right.$$
$$\left.+a_1^*\|\delta_\tau\overline{\boldsymbol{E}}_h^{n+\frac{1}{2}}\|^2\right] + \frac{b_2^*}{2}\delta_{2\tau}\|\boldsymbol{J}^{n+1}_{p,h}\|^2 + \sum_{k=0}^{2}\frac{\gamma}{\epsilon_0\omega_{pe}^2}\|\delta_\tau^k\overline{\boldsymbol{J}}_{d,h}^{n+\frac{[k+1]}{2}}\|^2 + b_1^*\|\delta_\tau\overline{\boldsymbol{J}}^{n+1}_{p,h}\|^2 + a_2^*\|\delta_\tau^2\overline{\boldsymbol{E}}_h^{n+\frac{1}{2}}\|^2$$
$$= -(\overline{\boldsymbol{J}}^{n+\frac{1}{2}}_{p,h}, \overline{\boldsymbol{E}}_h^{n+\frac{1}{2}}) - (\delta_\tau\overline{\boldsymbol{J}}^n_{p,h}, \delta_\tau\overline{\boldsymbol{E}}^n_h) + a_1^*(\delta_\tau\overline{\boldsymbol{J}}^{n+1}_{p,h}, \delta_\tau\overline{\boldsymbol{E}}_h^{n+1})$$
$$+\left(\frac{b_1^*}{2}(\delta_\tau\overline{\boldsymbol{J}}^{n+1}_{p,h} + \delta_\tau\overline{\boldsymbol{J}}^n_{p,h}) + b_2^*\overline{\overline{\boldsymbol{J}}}^{n+\frac{1}{2}}_{p,h} - a_0^*\overline{\boldsymbol{E}}_h^{n+\frac{1}{2}}, \delta_\tau^2\overline{\boldsymbol{E}}_h^{n+\frac{1}{2}}\right)$$
$$+(a_2^*\delta_\tau^2\boldsymbol{E}_h^{n+1} + a_0^*\boldsymbol{E}_h^{n+1}, \delta_\tau\overline{\boldsymbol{J}}^{n+1}_{p,h}), \tag{3.39}$$

which completes our proof. □

3.1. The discrete stability analysis

To prove a discrete stability, we need to use the following discrete Gronwall's inequality.

Lemma 3.1 (*[62, Lemma 1.4.2]*).
Assume that the sequence u_n satisfies

$$u_0 \leq g_0, \quad \text{and} \quad u_n \leq g_0 + r\tau \sum_{s=0}^{n-1} u_s, \ \forall\, n \geq 1,$$

for some positive constants g_0, r and τ. Then u_n satisfies

$$u_n \leq g_0 \cdot (1+r\tau)^n \leq g_0 \cdot \exp(rn\tau), \quad \forall\, n \geq 1.$$

Theorem 3.2. *Denote the discrete energy*

$$\begin{aligned} ENG_{cn}(m) := {} & \epsilon_0(\|\boldsymbol{E}_h^{m+1}\|^2 + \|\delta_\tau \boldsymbol{E}_h^{m+\frac{1}{2}}\|^2 + \|\delta_\tau^2 \boldsymbol{E}_h^{m+1}\|^2) \\ & + \mu_0(\|\boldsymbol{H}_h^{m+1}\|^2 + \|\delta_\tau \boldsymbol{H}_h^{m+\frac{1}{2}}\|^2 + \|\delta_\tau^2 \boldsymbol{H}_h^{m+1}\|^2) \\ & + \frac{1}{\epsilon_0\omega_{pe}^2}(\|\boldsymbol{J}_{d,h}^{m+1}\|^2 + \|\delta_\tau \boldsymbol{J}_{d,h}^{m+\frac{1}{2}}\|^2 + \|\delta_\tau^2 \boldsymbol{J}_{d,h}^{m+1}\|^2) + \|\delta_\tau \boldsymbol{J}_{p,h}^{m+\frac{3}{2}}\|^2 \\ & + a_1^*\|\delta_\tau \overline{\boldsymbol{E}}_h^{m+1}\|^2 + \frac{b_2^*}{2}(\|\boldsymbol{J}_{p,h}^{m+2}\|^2 + \|\boldsymbol{J}_{p,h}^{m+1}\|^2). \end{aligned} \tag{3.40}$$

Then under the time step constraint:

$$\tau \leq \tau_{cn} := \min\{\frac{1}{\frac{\sqrt{b_2^*}}{\sqrt{\epsilon_0}} + \frac{4b_2}{\epsilon_0}}, \ \frac{1}{\frac{1}{2} + \frac{|a_0^*|}{\epsilon_0} + \frac{4(a_0^*)^2}{\epsilon_0 b_1^*}}, \ \frac{2\sqrt{\epsilon_0}}{b_1^*}, \ \frac{b_1^*}{8a_1^*}, \ \frac{1}{\frac{b_1^*}{\sqrt{\epsilon_0}} + \frac{\sqrt{b_2^*}}{\sqrt{\epsilon_0}} + \frac{|a_0^*|}{\epsilon_0} + \frac{4(a_2^*)^2}{\epsilon_0 b_1^*}}\}, \tag{3.41}$$

we have: For any $m \geq 0$,

$$ENG_{cn}(m) \leq (ENG_{cn}(-1) + b_2^*\|\boldsymbol{J}_{p,h}^{-1}\|^2 + \|\delta_\tau \boldsymbol{J}_{p,h}^{-\frac{1}{2}}\|^2) \cdot \exp(C_{cn} m\tau), \tag{3.42}$$

where the positive constant C_{cn} depends on the physical parameters $\epsilon_0, a_0^*, a_1^*, a_2^*, b_1^*, b_2$.

Proof. Multiplying (3.25) by τ and dropping the nonnegative term $\sum_{k=0}^2 \frac{\gamma}{\epsilon_0\omega_{pe}^2}\|\delta_\tau^k \overline{\boldsymbol{J}}_{d,h}^{n+\frac{[k+1]}{2}}\|^2$ on the LHS of (3.25), then expanding those δ_τ terms explicitly, we have

$$\begin{aligned} & \frac{\epsilon_0}{2}\left[(\|\boldsymbol{E}_h^{n+1}\|^2 - \|\boldsymbol{E}_h^n\|^2) + (\|\delta_\tau \boldsymbol{E}_h^{n+\frac{1}{2}}\|^2 - \|\delta_\tau \boldsymbol{E}_h^{n-\frac{1}{2}}\|^2) + (\|\delta_\tau^2 \boldsymbol{E}_h^{n+1}\|^2 - \|\delta_\tau^2 \boldsymbol{E}_h^n\|^2)\right] \\ & + \frac{\mu_0}{2}\left[(\|\boldsymbol{H}_h^{n+1}\|^2 - \|\boldsymbol{H}_h^n\|^2) + (\|\delta_\tau \boldsymbol{H}_h^{n+\frac{1}{2}}\|^2 - \|\delta_\tau \boldsymbol{H}_h^{n-\frac{1}{2}}\|^2) + (\|\delta_\tau^2 \boldsymbol{H}_h^{n+1}\|^2 - \|\delta_\tau^2 \boldsymbol{H}_h^n\|^2)\right] \\ & + \frac{1}{2\epsilon_0\omega_{pe}^2}\left[(\|\boldsymbol{J}_{d,h}^{n+1}\|^2 - \|\boldsymbol{J}_{d,h}^n\|^2) + (\|\delta_\tau \boldsymbol{J}_{d,h}^{n+\frac{1}{2}}\|^2 - \|\delta_\tau \boldsymbol{J}_{d,h}^{n-\frac{1}{2}}\|^2) + (\|\delta_\tau^2 \boldsymbol{J}_{d,h}^{n+1}\|^2 - \|\delta_\tau^2 \boldsymbol{J}_{d,h}^n\|^2)\right] \\ & + \frac{1}{2}(\|\delta_\tau \boldsymbol{J}_{p,h}^{n+\frac{3}{2}}\|^2 - \|\delta_\tau \boldsymbol{J}_{p,h}^{n+\frac{1}{2}}\|^2) + \frac{a_1^*}{2}(\|\delta_\tau \overline{\boldsymbol{E}}_h^{n+1}\|^2 - \|\delta_\tau \overline{\boldsymbol{E}}_h^n\|^2) \\ & + \frac{b_2^*}{4}(\|\boldsymbol{J}_{p,h}^{n+2}\|^2 - \|\boldsymbol{J}_{p,h}^n\|^2) + \tau b_1^*\|\delta_\tau \overline{\boldsymbol{J}}_{p,h}^{n+1}\|^2 + \tau a_2^*\|\delta_\tau^2 \overline{\boldsymbol{E}}_h^{n+\frac{1}{2}}\|^2 \\ \leq {} & -\tau(\overline{\boldsymbol{J}}_{p,h}^{n+\frac{1}{2}}, \overline{\boldsymbol{E}}_h^{n+\frac{1}{2}}) - \tau(\delta_\tau \overline{\boldsymbol{J}}_{p,h}^n, \delta_\tau \overline{\boldsymbol{E}}_h^n) \\ & + \tau\left(\frac{b_1^*}{2}(\delta_\tau \overline{\boldsymbol{J}}_{p,h}^{n+1} + \delta_\tau \overline{\boldsymbol{J}}_{p,h}^n) + b_2^* \widetilde{\overline{\boldsymbol{J}}}_{p,h}^{n+\frac{1}{2}} - a_0^* \overline{\boldsymbol{E}}_h^{n+\frac{1}{2}}, \delta_\tau^2 \overline{\boldsymbol{E}}_h^{n+\frac{1}{2}}\right) \\ & + \tau(a_2^*\delta_\tau^2 \boldsymbol{E}_h^{n+1} + a_1^*\delta_\tau \overline{\boldsymbol{E}}_h^{n+1} + \tau a_0^* \boldsymbol{E}_h^{n+1}, \delta_\tau \overline{\boldsymbol{J}}_{p,h}^{n+1}). \end{aligned} \tag{3.43}$$

Note that all the terms on the RHS of (3.43) can be bounded by some corresponding terms on the LHS of (3.43) so that we can use the discrete Gronwall's inequality to prove the discrete stability. Below we show the details about how to bound each RHS term.

Using the Cauchy–Schwarz inequality, we have

$$
\begin{aligned}
&\tau(\overline{\boldsymbol{J}}_{p,h}^{n+\frac{1}{2}}, \overline{\boldsymbol{E}}_h^{n+\frac{1}{2}}) = \tau(\frac{\sqrt{b_2^*}}{\sqrt{b_2^*\epsilon_0}}\overline{\boldsymbol{J}}_{p,h}^{n+\frac{1}{2}}, \sqrt{\epsilon_0}\overline{\boldsymbol{E}}_h^{n+\frac{1}{2}})\\
&\leq \tau(\frac{b_2}{\epsilon_0}\cdot b_2^*\|\overline{\boldsymbol{J}}_{p,h}^{n+\frac{1}{2}}\|^2 + \frac{\epsilon_0}{4}\|\overline{\boldsymbol{E}}_h^{n+\frac{1}{2}}\|^2)\\
&\leq \tau\left[\frac{b_2}{\epsilon_0}\cdot\frac{b_2^*}{2}(\|\boldsymbol{J}_{p,h}^{n+1}\|^2 + \|\boldsymbol{J}_{p,h}^{n}\|^2) + \frac{\epsilon_0}{8}(\|\boldsymbol{E}_h^{n+1}\|^2 + \|\boldsymbol{E}_h^{n}\|^2)\right].
\end{aligned}
\tag{3.44}
$$

Similarly, we have

$$
\begin{aligned}
&\tau(\delta_\tau\overline{\boldsymbol{J}}_{p,h}^{n}, \delta_\tau\overline{\boldsymbol{E}}_h^{n}) = \frac{\tau}{\sqrt{a_1^*}}(\delta_\tau\overline{\boldsymbol{J}}_{p,h}^{n}, \sqrt{a_1^*}\delta_\tau\overline{\boldsymbol{E}}_h^{n})\\
&\leq \frac{\tau}{2\sqrt{a_1^*}}\left[\frac{1}{2}(\|\delta_\tau\boldsymbol{J}_{p,h}^{n+\frac{1}{2}}\|^2 + \|\delta_\tau\boldsymbol{J}_{p,h}^{n-\frac{1}{2}}\|^2) + a_1^*\|\delta_\tau\overline{\boldsymbol{E}}_h^{n}\|^2\right],
\end{aligned}
\tag{3.45}
$$

$$
\begin{aligned}
&\tau\left(\frac{b_1^*}{2}(\delta_\tau\overline{\boldsymbol{J}}_{p,h}^{n+1} + \delta_\tau\overline{\boldsymbol{J}}_{p,h}^{n}), \delta_\tau^2\overline{\boldsymbol{E}}_h^{n+\frac{1}{2}}\right)\\
&= \frac{\tau b_1^*}{2\sqrt{\epsilon_0}}(\delta_\tau\overline{\boldsymbol{J}}_{p,h}^{n+1}, \sqrt{\epsilon_0}\delta_\tau^2\overline{\boldsymbol{E}}_h^{n+\frac{1}{2}}) + \frac{\tau b_1^*}{2\sqrt{\epsilon_0}}(\delta_\tau\overline{\boldsymbol{J}}_{p,h}^{n}, \sqrt{\epsilon_0}\delta_\tau^2\overline{\boldsymbol{E}}_h^{n+\frac{1}{2}})\\
&\leq \frac{\tau b_1^*}{4\sqrt{\epsilon_0}}\left[\frac{1}{2}(\|\delta_\tau\boldsymbol{J}_{p,h}^{n+\frac{3}{2}}\|^2 + \|\delta_\tau\boldsymbol{J}_{p,h}^{n+\frac{1}{2}}\|^2) + \frac{\epsilon_0}{2}(\|\delta_\tau^2\boldsymbol{E}_h^{n+1}\|^2 + \|\delta_\tau^2\boldsymbol{E}_h^{n}\|^2)\right]\\
&\quad + \frac{\tau b_1^*}{4\sqrt{\epsilon_0}}\left[\frac{1}{2}(\|\delta_\tau\boldsymbol{J}_{p,h}^{n+\frac{1}{2}}\|^2 + \|\delta_\tau\boldsymbol{J}_{p,h}^{n-\frac{1}{2}}\|^2) + \frac{\epsilon_0}{2}(\|\delta_\tau^2\boldsymbol{E}_h^{n+1}\|^2 + \|\delta_\tau^2\boldsymbol{E}_h^{n}\|^2)\right],
\end{aligned}
\tag{3.46}
$$

$$
\begin{aligned}
&\tau\left(b_2^*\overline{\overline{\boldsymbol{J}}}_{p,h}^{n+\frac{1}{2}}, \delta_\tau^2\overline{\boldsymbol{E}}_h^{n+\frac{1}{2}}\right) \leq \frac{\tau\sqrt{b_2^*}}{2\sqrt{\epsilon_0}}(b_2^*\|\overline{\overline{\boldsymbol{J}}}_{p,h}^{n+\frac{1}{2}}\|^2 + \epsilon_0\|\delta_\tau^2\overline{\boldsymbol{E}}_h^{n+\frac{1}{2}}\|^2)\\
&\leq \frac{\tau\sqrt{b_2^*}}{2\sqrt{\epsilon_0}}\left[\frac{b_2^*}{4}(\|\boldsymbol{J}_{p,h}^{n+2}\|^2 + \|\boldsymbol{J}_{p,h}^{n+1}\|^2 + \|\boldsymbol{J}_{p,h}^{n}\|^2 + \|\boldsymbol{J}_{p,h}^{n-1}\|^2) + \frac{\epsilon_0}{2}(\|\delta_\tau^2\boldsymbol{E}_h^{n+1}\|^2 + \|\delta_\tau^2\boldsymbol{E}_h^{n}\|^2)\right],
\end{aligned}
\tag{3.47}
$$

$$
\begin{aligned}
&-\tau\left(a_0^*\overline{\boldsymbol{E}}_h^{n+\frac{1}{2}}, \delta_\tau^2\overline{\boldsymbol{E}}_h^{n+\frac{1}{2}}\right) \leq \frac{\tau|a_0^*|}{2\epsilon_0}\left(\epsilon_0\|\overline{\boldsymbol{E}}_h^{n+\frac{1}{2}}\|^2 + \epsilon_0\|\delta_\tau^2\overline{\boldsymbol{E}}_h^{n+\frac{1}{2}}\|^2\right)\\
&\leq \frac{\tau|a_0^*|}{2\epsilon_0}\left[\frac{\epsilon_0}{2}(\|\boldsymbol{E}_h^{n+1}\|^2 + \|\boldsymbol{E}_h^{n}\|^2) + \frac{\epsilon_0}{2}(\|\delta_\tau^2\boldsymbol{E}_h^{n+1}\|^2 + \|\delta_\tau^2\boldsymbol{E}_h^{n}\|^2)\right],
\end{aligned}
\tag{3.48}
$$

$$
\begin{aligned}
&\tau(a_2^*\delta_\tau^2\boldsymbol{E}_h^{n+1}, \delta_\tau\overline{\boldsymbol{J}}_{p,h}^{n+1}) = \tau(\frac{a_2^*}{\epsilon_0 b_1^*}\cdot\sqrt{\epsilon_0}\delta_\tau^2\boldsymbol{E}_h^{n+1}, \sqrt{b_1^*}\delta_\tau\overline{\boldsymbol{J}}_{p,h}^{n+1})\\
&\leq \frac{\tau(a_2^*)^2}{\epsilon_0 b_1^*}\cdot\epsilon_0\|\delta_\tau^2\boldsymbol{E}_h^{n+1}\|^2 + \frac{\tau}{4}\cdot b_1^*\|\delta_\tau\overline{\boldsymbol{J}}_{p,h}^{n+1}\|^2,
\end{aligned}
\tag{3.49}
$$

$$
\begin{aligned}
&\tau a_1^*(\delta_\tau\overline{\boldsymbol{J}}_{p,h}^{n+1}, \delta_\tau\overline{\boldsymbol{E}}_h^{n+1}) = \tau(\sqrt{b_1^*}\delta_\tau\overline{\boldsymbol{J}}_{p,h}^{n+1}, \frac{\sqrt{a_1^*}}{\sqrt{b_1^*}}\cdot\sqrt{a_1^*}\delta_\tau\overline{\boldsymbol{E}}_h^{n+1})\\
&\leq \tau(\frac{b_1^*}{8}\|\delta_\tau\overline{\boldsymbol{J}}_{p,h}^{n+1}\|^2 + \frac{2a_1^*}{b_1^*}\cdot a_1^*\|\delta_\tau\overline{\boldsymbol{E}}_h^{n+1}\|^2),
\end{aligned}
\tag{3.50}
$$

and

$$
\begin{aligned}
&\tau(a_0^*\boldsymbol{E}_h^{n+1}, \delta_\tau\overline{\boldsymbol{J}}_{p,h}^{n+1}) = \tau(\frac{a_0^*}{\sqrt{\epsilon_0 b_1^*}}\cdot\sqrt{\epsilon_0}\boldsymbol{E}_h^{n+1}, \sqrt{b_1^*}\delta_\tau\overline{\boldsymbol{J}}_{p,h}^{n+1})\\
&\leq \frac{\tau(a_0^*)^2}{\epsilon_0 b_1^*}\cdot\epsilon_0\|\boldsymbol{E}_h^{n+1}\|^2 + \frac{\tau b_1^*}{4}\|\delta_\tau\overline{\boldsymbol{J}}_{p,h}^{n+1}\|^2.
\end{aligned}
\tag{3.51}
$$

Substituting the above estimates (3.44)–(3.51) into (3.43), then summing up the result from $n = 0$ to any $m > 0$ and dropping the last two nonnegative terms on the LHS of (3.43), we finally have

$$
\begin{aligned}
&\frac{\epsilon_0}{2}\left[(\|\boldsymbol{E}_h^{m+1}\|^2 - \|\boldsymbol{E}_h^{0}\|^2) + (\|\delta_\tau\boldsymbol{E}_h^{m+\frac{1}{2}}\|^2 - \|\delta_\tau\boldsymbol{E}_h^{-\frac{1}{2}}\|^2) + (\|\delta_\tau^2\boldsymbol{E}_h^{m+1}\|^2 - \|\delta_\tau^2\boldsymbol{E}_h^{0}\|^2)\right]\\
&\quad + \frac{\mu_0}{2}\left[(\|\boldsymbol{H}_h^{m+1}\|^2 - \|\boldsymbol{H}_h^{0}\|^2) + (\|\delta_\tau\boldsymbol{H}_h^{m+\frac{1}{2}}\|^2 - \|\delta_\tau\boldsymbol{H}_h^{-\frac{1}{2}}\|^2) + (\|\delta_\tau^2\boldsymbol{H}_h^{m+1}\|^2 - \|\delta_\tau^2\boldsymbol{H}_h^{0}\|^2)\right]
\end{aligned}
$$

$$
\begin{aligned}
&+\frac{1}{2\epsilon_0\omega_{pe}^2}\left[(\|\boldsymbol{J}_{d,h}^{m+1}\|^2-\|\boldsymbol{J}_{d,h}^0\|^2)+(\|\delta_\tau\boldsymbol{J}_{d,h}^{m+\frac{1}{2}}\|^2-\|\delta_\tau\boldsymbol{J}_{d,h}^{-\frac{1}{2}}\|^2)+(\|\delta_\tau^2\boldsymbol{J}_{d,h}^{m+1}\|^2-\|\delta_\tau^2\boldsymbol{J}_{d,h}^0\|^2)\right]\\
&+\frac{1}{2}(\|\delta_\tau\boldsymbol{J}_{p,h}^{m+\frac{3}{2}}\|^2-\|\delta_\tau\boldsymbol{J}_{p,h}^{\frac{1}{2}}\|^2)+\frac{a_1^*}{2}(\|\delta_\tau\overline{\boldsymbol{E}}_h^{m+1}\|^2-\|\delta_\tau\overline{\boldsymbol{E}}_h^0\|^2)\\
&+\frac{b_2^*}{4}(\|\boldsymbol{J}_{p,h}^{m+2}\|^2+\|\boldsymbol{J}_{p,h}^{m+1}\|^2-\|\boldsymbol{J}_{p,h}^0\|^2-\|\boldsymbol{J}_{p,h}^1\|^2)\\
\le\ &\tau(\frac{\sqrt{b_2^*}}{2\sqrt{\epsilon_0}}+\frac{2b_2}{\epsilon_0})\frac{b_2^*}{4}(\|\boldsymbol{J}_{p,h}^{m+2}\|^2+\|\boldsymbol{J}_{p,h}^{m+1}\|^2)+\tau(\frac{\sqrt{b_2^*}}{2\sqrt{\epsilon_0}}+\frac{b_2}{\epsilon_0})\sum_{n=0}^m b_2^*\|\boldsymbol{J}_{p,h}^n\|^2\\
&+\frac{\tau\sqrt{b_2^*}}{2\sqrt{\epsilon_0}}\cdot\frac{b_2^*}{4}\|\boldsymbol{J}_{p,h}^{-1}\|^2+\tau[\frac{1}{8}+\frac{|a_0^*|}{4\epsilon_0}+\frac{(a_0^*)^2}{\epsilon_0 b_1^*}]\epsilon_0\|\boldsymbol{E}_h^{m+1}\|^2+\tau[\frac{1}{4}+\frac{|a_0^*|}{2\epsilon_0}+\frac{(a_0^*)^2}{\epsilon_0 b_1^*}]\sum_{n=0}^m\epsilon_0\|\boldsymbol{E}_h^n\|^2\\
&+\frac{\tau b_1^*}{8\sqrt{\epsilon_0}}\|\delta_\tau\boldsymbol{J}_{p,h}^{m+\frac{3}{2}}\|^2+\tau(\frac{1}{2\sqrt{a_1^*}}+\frac{b_1^*}{2\sqrt{\epsilon_0}})\sum_{n=0}^m\|\delta_\tau\boldsymbol{J}_{p,h}^{n+\frac{1}{2}}\|^2+\tau(\frac{1}{4\sqrt{a_1^*}}+\frac{b_1^*}{8\sqrt{\epsilon_0}})\|\delta_\tau\boldsymbol{J}_{p,h}^{-\frac{1}{2}}\|^2\\
&+\frac{\tau 2a_1^*}{b_1^*}\cdot a_1^*\|\delta_\tau\overline{\boldsymbol{E}}_h^{m+1}\|^2+\tau(\frac{1}{2\sqrt{a_1^*}}+\frac{2a_1^*}{b_1^*})\sum_{n=0}^m a_1^*\|\delta_\tau\overline{\boldsymbol{E}}_h^n\|^2\\
&+\tau(\frac{b_1^*}{4\sqrt{\epsilon_0}}+\frac{\sqrt{b_2^*}}{4\sqrt{\epsilon_0}}+\frac{|a_0^*|}{4\epsilon_0}+\frac{(a_2^*)^2}{\epsilon_0 b_1^*})\epsilon_0\|\delta_\tau^2\boldsymbol{E}_h^{m+1}\|^2\\
&+\tau(\frac{b_1^*}{2\sqrt{\epsilon_0}}+\frac{\sqrt{b_2^*}}{2\sqrt{\epsilon_0}}+\frac{|a_0^*|}{2\epsilon_0}+\frac{(a_2^*)^2}{\epsilon_0 b_1^*})\sum_{n=0}^m\epsilon_0\|\delta_\tau^2\boldsymbol{E}_h^n\|^2.
\end{aligned}
\tag{3.52}
$$

Finally, simply choosing the time step size τ to be bounded as follows:

$$
\begin{aligned}
&\tau(\frac{\sqrt{b_2^*}}{2\sqrt{\epsilon_0}}+\frac{2b_2}{\epsilon_0})\le\frac{1}{2},\quad \tau(\frac{1}{8}+\frac{|a_0^*|}{4\epsilon_0}+\frac{(a_0^*)^2}{\epsilon_0 b_1^*})\le\frac{1}{4},\quad \frac{\tau b_1^*}{8\sqrt{\epsilon_0}}\le\frac{1}{4},\\
&\frac{\tau 2a_1^*}{b_1^*}\le\frac{1}{4},\quad \tau(\frac{b_1^*}{4\sqrt{\epsilon_0}}+\frac{\sqrt{b_2^*}}{4\sqrt{\epsilon_0}}+\frac{|a_0^*|}{4\epsilon_0}+\frac{(a_2^*)^2}{\epsilon_0 b_1^*})\le\frac{1}{4},
\end{aligned}
\tag{3.53}
$$

which are equivalent to the constraint (3.41), then using the discrete Gronwall's inequality to (3.52), we complete our proof. □

3.2. The error estimate analysis

To carry out the error analysis, we introduce the notation Π_c and Π_2 for the standard Nédélec interpolation in space $\boldsymbol{V}_h$ and the standard L^2 projection onto space U_h, respectively. It is known that the following interpolation and projection errors hold true (cf. [55,56]):

$$\|\boldsymbol{u}-\Pi_c\boldsymbol{u}\|_{H(\mathrm{curl};\Omega)}\le ch^p\|\boldsymbol{u}\|_{H^p(\mathrm{curl};\Omega)},\quad\forall\,\boldsymbol{u}\in H^p(\mathrm{curl};\Omega),\tag{3.54}$$

$$\|u-\Pi_2 u\|_{L^2(\Omega)}\le ch^p\|u\|_{H^p(\Omega)},\quad\forall\,u\in H^p(\Omega),\tag{3.55}$$

where we denote the norm $\|u\|_{H^p(\Omega)}$ for the Sobolev space $H^p(\Omega)$, and norm $\|\boldsymbol{u}\|_{H^s(\mathrm{curl};\Omega)}:=(\|\boldsymbol{u}\|^2_{(H^s(\Omega))^2}+\|\nabla\times\boldsymbol{u}\|^2_{H^s(\Omega)})^{1/2}$ for the Sobolev space

$$H^s(\mathrm{curl};\Omega)=\{\boldsymbol{u}\in(H^s(\Omega))^2\mid\nabla\times\boldsymbol{u}\in H^s(\Omega)\}.$$

Integrating (2.1) with respect to t from t_n to t_{n+1}, dividing the result by τ, then multiplying by ϕ_h and integrating over Ω, we obtain: For any $\phi_h\in\boldsymbol{V}_h^0$,

$$\epsilon_0(\delta_\tau\boldsymbol{E}(t_{n+\frac{1}{2}}),\phi_h)=(\frac{1}{\tau}\int_{t_n}^{t_{n+1}}\boldsymbol{H}(s)ds,\nabla\times\phi_h)-(\frac{1}{\tau}\int_{t_n}^{t_{n+1}}(\boldsymbol{J}_d(s)+\boldsymbol{J}_p(s))ds,\phi_h).\tag{3.56}$$

Subtracting (3.56) from (3.19), we obtain the error equation

$$
\begin{aligned}
\epsilon_0(\delta_\tau\mathcal{E}_h^{n+\frac{1}{2}},\phi_h)=&\left(\overline{\mathcal{H}}_h^{n+\frac{1}{2}}+(\overline{\boldsymbol{H}}(t_{n+\frac{1}{2}})-\frac{1}{\tau}\int_{t_n}^{t_{n+1}}\boldsymbol{H}(s)ds),\nabla\times\phi_h\right)-(\overline{\mathcal{J}}_{d,h}^{n+\frac{1}{2}}+\overline{\mathcal{J}}_{p,h}^{n+\frac{1}{2}},\phi_h)\\
&-\left(\bar{\boldsymbol{J}}_d(t_{n+\frac{1}{2}})+\bar{\boldsymbol{J}}_p(t_{n+\frac{1}{2}})-\frac{1}{\tau}\int_{t_n}^{t_{n+1}}(\boldsymbol{J}_d(s)+\boldsymbol{J}_p(s))ds,\phi_h\right),
\end{aligned}
\tag{3.57}
$$

where we used the following error notation:

$$\mathcal{E}_h^n:=\boldsymbol{E}_h^n-\boldsymbol{E}(t_n)=\left(\boldsymbol{E}_h^n-\Pi_c\boldsymbol{E}(t_n)\right)-(\boldsymbol{E}(t_n)-\Pi_c\boldsymbol{E}(t_n)):=\mathcal{E}_{h\xi}^n-\mathcal{E}_{h\eta}^n,\tag{3.58}$$

where for simplicity we denote $\boldsymbol{E}(t_n)=\boldsymbol{E}(\boldsymbol{x},t_n)$, and split the error between the FE solution and the exact solution into two parts, i.e., $\mathcal{E}_{h\xi}^n \in \boldsymbol{V}_h^0$ (the error between the FE solution and interpolation of the exact solution) and $\mathcal{E}_{h\eta}^n$ (the interpolation error).

Similarly, we adopt the following error notation:

$$\mathcal{H}_h^n := \boldsymbol{H}_h^n - \boldsymbol{H}(t_n) = \left(\boldsymbol{H}_h^n - \Pi_2\boldsymbol{H}(t_n)\right) - (\boldsymbol{H}(t_n) - \Pi_2\boldsymbol{H}(t_n)) := \mathcal{H}_{h\xi}^n - \mathcal{H}_{h\eta}^n, \tag{3.59}$$

$$\mathcal{J}_{d,h}^n := \boldsymbol{J}_{d,h}^n - \boldsymbol{J}_d(t_n) = \left(\boldsymbol{J}_{d,h}^n - \Pi_c\boldsymbol{J}_d(t_n)\right) - (\boldsymbol{J}_d(t_n) - \Pi_c\boldsymbol{J}_d(t_n)) := \mathcal{J}_{d\xi}^n - \mathcal{J}_{d\eta}^n, \tag{3.60}$$

$$\mathcal{J}_{p,h}^n := \boldsymbol{J}_{p,h}^n - \boldsymbol{J}_p(t_n) = \left(\boldsymbol{J}_{p,h}^n - \Pi_c\boldsymbol{J}_p(t_n)\right) - \left(\boldsymbol{J}_p(t_n) - \Pi_c\boldsymbol{J}_p(t_n)\right) := \mathcal{J}_{p\xi}^n - \mathcal{J}_{p\eta}^n. \tag{3.61}$$

Using the above error notation in (3.57), we can obtain the E-error equation:

$$\begin{aligned}
&\epsilon_0(\delta_\tau\mathcal{E}_{h\xi}^{n+\frac12},\phi_h) - (\overline{\mathcal{H}}_{h\xi}^{n+\frac12},\nabla\times\phi_h) + (\overline{\mathcal{J}}_{d\xi}^{n+\frac12} + \overline{\mathcal{J}}_{p\xi}^{n+\frac12},\phi_h)\\
&= \epsilon_0(\delta_\tau\mathcal{E}_{h\eta}^{n+\frac12},\phi_h) - (\overline{\mathcal{H}}_{h\eta}^{n+\frac12},\nabla\times\phi_h) + (\overline{\mathcal{J}}_{d\eta}^{n+\frac12} + \overline{\mathcal{J}}_{p\eta}^{n+\frac12},\phi_h)\\
&\quad + \left(\overline{\boldsymbol{H}}(t_{n+\frac12}) - \frac{1}{\tau}\int_{t_n}^{t_{n+1}}\boldsymbol{H}(s)ds,\nabla\times\phi_h\right)\\
&\quad - \left(\bar{\boldsymbol{J}}_d(t_{n+\frac12}) + \bar{\boldsymbol{J}}_p(t_{n+\frac12}) - \frac{1}{\tau}\int_{t_n}^{t_{n+1}}(\boldsymbol{J}_d(s)+\boldsymbol{J}_p(s))ds,\phi_h\right).
\end{aligned} \tag{3.62}$$

Integrating (2.2) with respect to t from t_n to t_{n+1}, dividing the result by τ, then multiplying by ψ_h and integrating over Ω, we obtain: For any $\psi_h \in \boldsymbol{U}_h$,

$$\mu_0(\delta_\tau\boldsymbol{H}(t_{n+\frac12}),\psi_h) = -(\frac{1}{\tau}\int_{t_n}^{t_{n+1}}\nabla\times\boldsymbol{E}(s)ds,\psi_h). \tag{3.63}$$

Subtracting (3.63) from (3.20), we obtain the error equation

$$\mu_0(\delta_\tau\mathcal{H}_h^{n+\frac12},\psi_h) = -(\nabla\times\overline{\mathcal{E}}_h^{n+\frac12},\psi_h) - (\nabla\times\overline{\boldsymbol{E}}(t_{n+\frac12}) - \frac{1}{\tau}\int_{t_n}^{t_{n+1}}\nabla\times\boldsymbol{E}(s)ds,\psi_h). \tag{3.64}$$

By splitting the errors in (3.64), we obtain the H-error equation:

$$\begin{aligned}
&\mu_0(\delta_\tau\mathcal{H}_{h\xi}^{n+\frac12},\psi_h) + (\nabla\times\overline{\mathcal{E}}_{h\xi}^{n+\frac12},\psi_h) = \mu_0(\delta_\tau\mathcal{H}_{h\eta}^{n+\frac12},\psi_h) + (\nabla\times\overline{\mathcal{E}}_{h\eta}^{n+\frac12},\psi_h)\\
&\quad -(\nabla\times\overline{\boldsymbol{E}}(t_{n+\frac12}) - \frac{1}{\tau}\int_{t_n}^{t_{n+1}}\nabla\times\boldsymbol{E}(s)ds,\psi_h).
\end{aligned} \tag{3.65}$$

By the same technique, we can obtain the J_d-error equation:

$$\begin{aligned}
&(\frac{1}{\epsilon_0\omega_{pe}^2}\delta_\tau\mathcal{J}_{d\xi}^{n+\frac12} + \frac{\gamma}{\epsilon_0\omega_{pe}^2}\overline{\mathcal{J}}_{d\xi}^{n+\frac12} - \overline{\mathcal{E}}_{h\xi}^{n+\frac12},\phi_h) = (\frac{1}{\epsilon_0\omega_{pe}^2}\delta_\tau\mathcal{J}_{d\eta}^{n+\frac12} + \frac{\gamma}{\epsilon_0\omega_{pe}^2}\overline{\mathcal{J}}_{d\eta}^{n+\frac12} - \overline{\mathcal{E}}_{h\eta}^{n+\frac12},\phi_h)\\
&\quad + \frac{\gamma}{\epsilon_0\omega_{pe}^2}(\frac{1}{\tau}\int_{t_n}^{t_{n+1}}\boldsymbol{J}_d(s)ds - \bar{\boldsymbol{J}}_d(t_{n+\frac12}),\phi_h) + (\overline{\boldsymbol{E}}(t_{n+\frac12}) - \frac{1}{\tau}\int_{t_n}^{t_{n+1}}\boldsymbol{E}(s)ds,\phi_h),
\end{aligned} \tag{3.66}$$

and the J_p-error equation:

$$\begin{aligned}
&(\delta_\tau^2\mathcal{J}_{p\xi}^n + b_1^*\delta_{2\tau}\mathcal{J}_{p\xi}^n + b_2^*\widetilde{\mathcal{J}}_{p\xi}^n - a_2^*\delta_\tau^2\mathcal{E}_{h\xi}^n - a_1^*\delta_{2\tau}\mathcal{E}_{h\xi}^n - a_0^*\mathcal{E}_{h\xi}^n,\phi_h)\\
&= (\delta_\tau^2\mathcal{J}_{p\eta}^n + b_1^*\delta_{2\tau}\mathcal{J}_{p\eta}^n + b_2^*\widetilde{\mathcal{J}}_{p\eta}^n - a_2^*\delta_\tau^2\mathcal{E}_{h\eta}^n - a_1^*\delta_{2\tau}\mathcal{E}_{h\eta}^n - a_0^*\mathcal{E}_{h\eta}^n,\phi_h)\\
&\quad + \left([\delta_{2\tau}(\partial_t\boldsymbol{J}_p(t_n)) - \delta_\tau^2\boldsymbol{J}_p(t_n)] + b_2^*[\frac{1}{2\tau}\int_{t_{n-1}}^{t_{n+1}}\boldsymbol{J}_p(s)ds - \widetilde{\boldsymbol{J}}_p(t_n)],\phi_h\right)\\
&\quad - \left(a_2^*[\delta_{2\tau}(\partial_t\boldsymbol{E}(t_n)) - \delta_\tau^2\boldsymbol{E}(t_n)] + a_0^*[\frac{1}{2\tau}\int_{t_{n-1}}^{t_{n+1}}\boldsymbol{E}(s)ds - \boldsymbol{E}(t_n)],\phi_h\right).
\end{aligned} \tag{3.67}$$

With the establishment of the above error equations, we can obtain the following optimal error estimate for the CN scheme (3.19)–(3.22).

Theorem 3.3. *Under the same time step constraint as given in Theorem 3.2, we have: For any $m \geq 0$,*

$$\begin{aligned}
&\epsilon_0(\|\boldsymbol{E}_h^{m+1} - \boldsymbol{E}(t_{m+1})\|^2 + \|\delta_\tau\boldsymbol{E}_h^{m+\frac12} - \partial_t\boldsymbol{E}(t_{m+\frac12})\|^2 + \|\delta_\tau^2\boldsymbol{E}_h^{m+1} - \partial_{t^2}\boldsymbol{E}(t_{m+1})\|^2)\\
&+ \mu_0(\|\boldsymbol{H}_h^{m+1} - \boldsymbol{H}(t_{m+1})\|^2 + \|\delta_\tau\boldsymbol{H}_h^{m+\frac12} - \partial_t\boldsymbol{H}(t_{m+\frac12})\|^2 + \|\delta_\tau^2\boldsymbol{H}_h^{m+1} - \partial_{t^2}\boldsymbol{H}(t_{m+1})\|^2)
\end{aligned}$$

$$+\frac{1}{\epsilon_0\omega_{pe}^2}(\|\boldsymbol{J}_{d,h}^{m+1}-\boldsymbol{J}_d(t_{m+1})\|^2+\|\delta_\tau\boldsymbol{J}_{d,h}^{m+\frac{1}{2}}-\partial_t\boldsymbol{J}_d(t_{m+\frac{1}{2}})\|^2+\|\delta_\tau^2\boldsymbol{J}_{d,h}^{m+1}-\partial_{t^2}\boldsymbol{J}_d(t_{m+1})\|^2)$$
$$+\|\delta_\tau\boldsymbol{J}_{p,h}^{m+\frac{3}{2}}-\partial_t\boldsymbol{J}_p(t_{m+\frac{3}{2}})\|^2+a_1^*\|\delta_\tau\overline{\boldsymbol{E}}_h^{m+1}-\partial_t\overline{\boldsymbol{E}}(t_{m+1})\|^2$$
$$+\frac{b_2^*}{2}(\|\boldsymbol{J}_{p,h}^{m+2}-\boldsymbol{J}_p(t_{m+2})\|^2+\|\boldsymbol{J}_{p,h}^{m+1}-\boldsymbol{J}_p(t_{m+1})\|^2)\le C(h^p+\tau^2)^2, \tag{3.68}$$

where $p\ge 1$ is the degree of the FE basis functions in $\boldsymbol{V}_h^0$ and $\boldsymbol{U}_h$, and the positive constant C depends on the physical parameters $\epsilon_0, a_0^*, a_1^*, a_2^*, b_1^*, b_2$, but is independent of h and τ.

Proof. Note that all LHS terms in the error Eqs. (3.62), (3.65), (3.66) and (3.67) have exactly the same form as the scheme (3.19)–(3.22), while all RHS terms can be easily shown to be bounded by $O(h^p+\tau^2)$ in the L^2-norm.

Then by following exactly the same techniques developed for proving the numerical stability in Theorem 3.2, we have: For any $m\ge 0$,

$$\epsilon_0(\|\mathcal{E}_{h\xi}^{m+1}\|^2+\|\delta_\tau\mathcal{E}_{h\xi}^{m+\frac{1}{2}}\|^2+\|\delta_\tau^2\mathcal{E}_{h\xi}^{m+1}\|^2)$$
$$+\mu_0(\|\mathcal{H}_{h\xi}^{m+1}\|^2+\|\delta_\tau\mathcal{H}_{h\xi}^{m+\frac{1}{2}}\|^2+\|\delta_\tau^2\mathcal{H}_{h\xi}^{m+1}\|^2)$$
$$+\frac{1}{\epsilon_0\omega_{pe}^2}(\|\mathcal{J}_{d\xi}^{m+1}\|^2+\|\delta_\tau\mathcal{J}_{d\xi}^{m+\frac{1}{2}}\|^2+\|\delta_\tau^2\mathcal{J}_{d\xi}^{m+1}\|^2)+\|\delta_\tau\mathcal{J}_{p\xi}^{m+\frac{3}{2}}\|^2$$
$$+a_1^*\|\delta_\tau\overline{\mathcal{E}}_{h\xi}^{m+1}\|^2+\frac{b_2^*}{2}(\|\mathcal{J}_{p\xi}^{m+2}\|^2+\|\mathcal{J}_{p\xi}^{m+1}\|^2)\le C(h^p+\tau^2)^2. \tag{3.69}$$

Finally, using the triangle inequality, the estimate (3.69), the interpolation and projection error estimates (3.54)–(3.55), we can conclude the proof. For illustration, we have

$$\|\boldsymbol{E}_h^{m+1}-\boldsymbol{E}(t_{m+1})\|^2=\|(\boldsymbol{E}_h^{m+1}-\Pi_c\boldsymbol{E}(t_{m+1}))+(\Pi_c-I)\boldsymbol{E}(t_{m+1})\|^2$$
$$\le 2[\|\mathcal{E}_{h\xi}^{m+1}\|^2+\|(\Pi_c-I)\boldsymbol{E}(t_{m+1})\|^2]$$
$$\le C(\tau^4+h^{2p})+Ch^{2p}\|\boldsymbol{E}\|^2_{C([0,T];H^p(curl;\Omega))},$$

where we used the estimate (3.69) and the interpolation error estimate (3.54).

Similarly, we have

$$\|\delta_\tau\boldsymbol{E}_h^{m+\frac{1}{2}}-\partial_t\boldsymbol{E}(t_{m+\frac{1}{2}})\|^2=\|\delta_\tau\mathcal{E}_{h\xi}^{m+\frac{1}{2}}+\delta_\tau(\Pi_c-I)\boldsymbol{E}(t_{m+\frac{1}{2}})+\delta_\tau\boldsymbol{E}(t_{m+\frac{1}{2}})-\partial_t\boldsymbol{E}(t_{m+\frac{1}{2}})\|^2$$
$$\le 3[\|\delta_\tau\mathcal{E}_{h\xi}^{m+\frac{1}{2}}\|^2+\frac{1}{\tau}\int_{t_m}^{t_{m+1}}\|\partial_t(\Pi_c-I)\boldsymbol{E}(s)\|^2ds+\|\delta_\tau\boldsymbol{E}(t_{m+\frac{1}{2}})-\partial_t\boldsymbol{E}(t_{m+\frac{1}{2}})\|^2]$$
$$\le C(\tau^4+h^{2p})+Ch^{2p}\|\partial_t\boldsymbol{E}\|^2_{C([0,T];H^p(curl;\Omega))}+C\tau^4\|\partial_{t^3}\boldsymbol{E}\|^2_{C([0,T];H^p(curl;\Omega))},$$

where we used the estimate (3.69), the interpolation error estimate (3.54) and Lemma 3.16 of [56]. □

4. The leap-frog scheme and its analysis

Using the time staggering for approximating electric and magnetic fields, we can develop the following leap-frog scheme for (2.1)–(2.4): Given proper initial approximations $(\boldsymbol{E}_h^0,\boldsymbol{E}_h^{-1},\boldsymbol{J}_{d,h}^{-\frac{1}{2}},\boldsymbol{J}_{p,h}^0,\boldsymbol{J}_{p,h}^{-1},\boldsymbol{H}_h^{-\frac{1}{2}})$, for any $n\ge 0$, solve for $(\boldsymbol{E}_h^{n+1},\boldsymbol{J}_{d,h}^{n+\frac{1}{2}},\boldsymbol{J}_{p,h}^{n+1},\boldsymbol{H}_h^{n+\frac{1}{2}})\in(\boldsymbol{V}_h^0)^3\times U_h$ satisfying the following:

$$\epsilon_0(\delta_\tau\boldsymbol{E}_h^{n+\frac{1}{2}},\phi_h)=(\boldsymbol{H}_h^{n+\frac{1}{2}},\nabla\times\phi_h)-(\boldsymbol{J}_{d,h}^{n+\frac{1}{2}},\phi_h)-(\overline{\boldsymbol{J}}_{p,h}^{n+\frac{1}{2}},\phi_h), \tag{4.70}$$
$$\mu_0(\delta_\tau\boldsymbol{H}_h^n,\psi_h)=-(\nabla\times\boldsymbol{E}_h^n,\psi_h), \tag{4.71}$$
$$(\frac{1}{\epsilon_0\omega_{pe}^2}\delta_\tau\boldsymbol{J}_{d,h}^n+\frac{\gamma}{\epsilon_0\omega_{pe}^2}\overline{\boldsymbol{J}}_{d,h}^n,\phi_h)=(\boldsymbol{E}_h^n,\phi_h) \tag{4.72}$$
$$(\delta_\tau^2\boldsymbol{J}_{p,h}^n+b_1^*\delta_{2\tau}\boldsymbol{J}_{p,h}^n+b_2^*\widetilde{\boldsymbol{J}}_{p,h}^n,\phi_h)=(a_2^*\delta_\tau^2\boldsymbol{E}_h^n+a_1^*\delta_{2\tau}\boldsymbol{E}_h^n+a_0^*\boldsymbol{E}_h^n,\phi_h), \tag{4.73}$$

for any $\phi_h\in\boldsymbol{V}_h^0$ and $\psi_h\in U_h$. The initial conditions (2.7)–(2.8) are discretized as follows:

$$\boldsymbol{E}_h^0=\Pi_c\boldsymbol{E}_0(\boldsymbol{x}),\ \frac{\boldsymbol{H}_h^{\frac{1}{2}}+\boldsymbol{H}_h^{-\frac{1}{2}}}{2}=\Pi_2\boldsymbol{H}_0(\boldsymbol{x}),\ \frac{\boldsymbol{J}_{d,h}^{\frac{1}{2}}+\boldsymbol{J}_{d,h}^{-\frac{1}{2}}}{2}=\Pi_c\boldsymbol{J}_{d0}(\boldsymbol{x}),\ \boldsymbol{J}_{p,h}^0=\Pi_c\boldsymbol{J}_{p0}(\boldsymbol{x}), \tag{4.74}$$
$$\delta_{2\tau}\boldsymbol{E}_h^0:=\frac{\boldsymbol{E}_h^1-\boldsymbol{E}_h^{-1}}{2\tau}=\Pi_c\boldsymbol{E}_1(\boldsymbol{x}),\quad \delta_{2\tau}\boldsymbol{J}_{p,h}^0:=\frac{\boldsymbol{J}_{p,h}^1-\boldsymbol{J}_{p,h}^{-1}}{2\tau}=\Pi_c\boldsymbol{J}_{p1}(\boldsymbol{x}), \tag{4.75}$$

We can establish the following conditional stability for our leap-frog scheme.

Theorem 4.1. *Denote $C_v = 1/\sqrt{\epsilon_0\mu_0}$ for the wave speed in vacuum, $C_{inv} > 0$ for the constant in the standard inverse estimate [39]:*

$$\|\nabla\times\boldsymbol{v}_h\| \le C_{inv}h^{-1}\|\boldsymbol{v}_h\|, \quad \forall \boldsymbol{v}_h\in\boldsymbol{V}_h, \tag{4.76}$$

and the discrete energy

$$\begin{aligned} ENG_{lf}(m) := {}& \epsilon_0(\|\boldsymbol{E}_h^{m+1}\|^2 + \|\delta_\tau\boldsymbol{E}_h^{m+\frac12}\|^2 + \|\delta_\tau^2\boldsymbol{E}_h^{m+1}\|^2) \\ &+ \mu_0(\|\boldsymbol{H}_h^{m+\frac12}\|^2 + \|\delta_\tau\boldsymbol{H}_h^{m+1}\|^2 + \|\delta_\tau^2\boldsymbol{H}_h^{m+\frac12}\|^2) \\ &+ \frac{1}{\epsilon_0\omega_{pe}^2}(\|\boldsymbol{J}_{d,h}^{m+\frac12}\|^2 + \|\delta_\tau\boldsymbol{J}_{d,h}^{m+1}\|^2 + \|\delta_\tau^2\boldsymbol{J}_{d,h}^{m+\frac12}\|^2) \\ &+ \|\delta_\tau\boldsymbol{J}_{p,h}^{m+\frac32}\|^2 + a_1^*\|\delta_\tau\overline{\boldsymbol{E}}_h^{m+1}\|^2 + \frac{b_2^*}{2}(\|\boldsymbol{J}_{p,h}^{m+2}\|^2 + \|\boldsymbol{J}_{p,h}^{m+1}\|^2). \end{aligned} \tag{4.77}$$

Then under the time step constraint:

$$\tau \le \tau_{lf} := \min\{\tau_{cn}, \frac{h}{2C_vC_{inv}}, \frac{1}{2\omega_{pe}}\}, \tag{4.78}$$

we have: For any $m \ge 0$,

$$ENG_{lf}(m) \le (ENG_{lf}(-1) + b_2^*\|\boldsymbol{J}_{p,h}^{-1}\|^2 + \|\delta_\tau\boldsymbol{J}_{p,h}^{-\frac12}\|^2)\cdot\exp(C_{lf}m\tau), \tag{4.79}$$

where the positive constant C_{lf} depends on the physical parameters $\epsilon_0, a_0^*, a_1^*, a_2^*, b_1^*, b_2, \omega_{pe}$.

Proof. Considering that the proof is lengthy and technical, we break the proof into several major steps to make it easy to follow.

(I) Choosing $\phi_h = \tau\overline{\boldsymbol{E}}_h^{n+\frac12}$, $\psi_h = \tau\overline{\boldsymbol{H}}_h^n$, and $\phi_h = \tau\overline{\boldsymbol{J}}_{d,h}^n$ in (4.70), (4.71), and (4.72), respectively, then summing up the results, we have

$$\begin{aligned} &\frac{\epsilon_0}{2}(\|\boldsymbol{E}_h^{n+1}\|^2 - \|\boldsymbol{E}_h^n\|^2) + \frac{\mu_0}{2}(\|\boldsymbol{H}_h^{n+\frac12}\|^2 - \|\boldsymbol{H}_h^{n-\frac12}\|^2) \\ &\quad + \frac{1}{2\epsilon_0\omega_{pe}^2}(\|\boldsymbol{J}_{d,h}^{n+\frac12}\|^2 - \|\boldsymbol{J}_{d,h}^{n-\frac12}\|^2) + \frac{\tau\gamma}{\epsilon_0\omega_{pe}^2}\|\overline{\boldsymbol{J}}_{d,h}^n\|^2 \\ &= \frac{\tau}{2}\left[(\boldsymbol{H}_h^{n+\frac12}, \nabla\times\boldsymbol{E}_h^{n+1}) - (\boldsymbol{H}_h^{n-\frac12}, \nabla\times\boldsymbol{E}_h^n)\right] - \tau(\overline{\boldsymbol{J}}_{p,h}^{n+\frac12}, \overline{\boldsymbol{E}}_h^{n+\frac12}) \\ &\quad - \frac{\tau}{2}\left[(\boldsymbol{J}_{d,h}^{n+\frac12}, \boldsymbol{E}_h^{n+1}) - (\boldsymbol{J}_{d,h}^{n-\frac12}, \boldsymbol{E}_h^n)\right], \end{aligned} \tag{4.80}$$

where we used the following identities

$$(\boldsymbol{H}_h^{n+\frac12}, \nabla\times\overline{\boldsymbol{E}}_h^{n+\frac12}) - (\nabla\times\boldsymbol{E}_h^n, \overline{\boldsymbol{H}}_h^n) = \frac12\left[(\boldsymbol{H}_h^{n+\frac12}, \nabla\times\boldsymbol{E}_h^{n+1}) - (\boldsymbol{H}_h^{n-\frac12}, \nabla\times\boldsymbol{E}_h^n)\right]$$

and

$$(\boldsymbol{J}_{d,h}^{n+\frac12}, \overline{\boldsymbol{E}}_h^{n+\frac12}) - (\boldsymbol{E}_h^n, \overline{\boldsymbol{J}}_{d,h}^n) = \frac12\left[(\boldsymbol{J}_{d,h}^{n+\frac12}, \boldsymbol{E}_h^{n+1}) - (\boldsymbol{J}_{d,h}^{n-\frac12}, \boldsymbol{E}_h^n)\right].$$

(II) Using (4.70) to subtract itself with n replaced by $n-1$, we obtain

$$\epsilon_0(\delta_\tau^2\boldsymbol{E}_h^n, \phi_h) = (\delta_\tau\boldsymbol{H}_h^n, \nabla\times\phi_h) - (\delta_\tau\boldsymbol{J}_{d,h}^n, \phi_h) - (\delta_\tau\overline{\boldsymbol{J}}_{p,h}^n, \phi_h), \tag{4.81}$$

Using (4.71) with n replaced by $n+1$ to subtract itself, we have

$$\mu_0(\delta_\tau^2\boldsymbol{H}_h^{n+\frac12}, \psi_h) = -(\nabla\times\delta_\tau\boldsymbol{E}_h^{n+\frac12}, \psi_h). \tag{4.82}$$

Using (4.72) with n increased to $n+1$ to subtract itself, we have

$$(\frac{1}{\epsilon_0\omega_{pe}^2}\delta_\tau^2\boldsymbol{J}_{d,h}^{n+\frac12} + \frac{\gamma}{\epsilon_0\omega_{pe}^2}\delta_\tau\overline{\boldsymbol{J}}_{d,h}^{n+\frac12}, \phi_h) = (\delta_\tau\boldsymbol{E}_h^{n+\frac12}, \phi_h). \tag{4.83}$$

Choosing $\phi_h = \tau\delta_\tau\overline{\boldsymbol{E}}_h^n$, $\psi_h = \tau\delta_\tau\overline{\boldsymbol{H}}_h^{n+\frac{1}{2}}$, and $\phi_h = \tau\delta_\tau\overline{\boldsymbol{J}}_{d,h}^{n+\frac{1}{2}}$ in (4.81), (4.82), and (4.83), respectively, and summing up the results, we have

$$\begin{aligned}&\frac{\epsilon_0}{2}(\|\delta_\tau\boldsymbol{E}_h^{n+\frac{1}{2}}\|^2-\|\delta_\tau\boldsymbol{E}_h^{n-\frac{1}{2}}\|^2)+\frac{\mu_0}{2}(\|\delta_\tau\boldsymbol{H}_h^{n+1}\|^2-\|\delta_\tau\boldsymbol{H}_h^{n}\|^2)\\&\quad+\frac{1}{2\epsilon_0\omega_{pe}^2}(\|\delta_\tau\boldsymbol{J}_{d,h}^{n+1}\|^2-\|\delta_\tau\boldsymbol{J}_{d,h}^{n}\|^2)+\frac{\tau\gamma}{\epsilon_0\omega_{pe}^2}\|\delta_\tau\overline{\boldsymbol{J}}_{d,h}^{n+\frac{1}{2}}\|^2\\&=\frac{\tau}{2}\left[(\delta_\tau\boldsymbol{H}_h^n,\nabla\times\delta_\tau\boldsymbol{E}_h^{n-\frac{1}{2}})-(\delta_\tau\boldsymbol{H}_h^{n+1},\nabla\times\delta_\tau\boldsymbol{E}_h^{n+\frac{1}{2}})\right]-\tau(\delta_\tau\overline{\boldsymbol{J}}_{p,h}^n,\delta_\tau\overline{\boldsymbol{E}}_h^n)\\&\quad+\frac{\tau}{2}\left[(\delta_\tau\boldsymbol{J}_{d,h}^{n+1},\delta_\tau\boldsymbol{E}_h^{n+\frac{1}{2}})-(\delta_\tau\boldsymbol{J}_{d,h}^{n},\delta_\tau\boldsymbol{E}_h^{n-\frac{1}{2}})\right],\end{aligned}\tag{4.84}$$

where we used the following identities

$$\begin{aligned}&(\delta_\tau\boldsymbol{H}_h^n,\nabla\times\delta_\tau\overline{\boldsymbol{E}}_h^n)-(\nabla\times\delta_\tau\boldsymbol{E}_h^{n+\frac{1}{2}},\delta_\tau\overline{\boldsymbol{H}}_h^{n+\frac{1}{2}})\\&=\frac{1}{2}\left[(\delta_\tau\boldsymbol{H}_h^n,\nabla\times\delta_\tau\boldsymbol{E}_h^{n-\frac{1}{2}})-(\delta_\tau\boldsymbol{H}_h^{n+1},\nabla\times\delta_\tau\boldsymbol{E}_h^{n+\frac{1}{2}})\right]\end{aligned}$$

and

$$(\delta_\tau\overline{\boldsymbol{J}}_{d,h}^{n+\frac{1}{2}},\delta_\tau\boldsymbol{E}_h^{n+\frac{1}{2}})-(\delta_\tau\overline{\boldsymbol{E}}_h^n,\delta_\tau\boldsymbol{J}_{d,h}^n)=\frac{1}{2}\left[(\delta_\tau\boldsymbol{J}_{d,h}^{n+1},\delta_\tau\boldsymbol{E}_h^{n+\frac{1}{2}})-(\delta_\tau\boldsymbol{J}_{d,h}^{n},\delta_\tau\boldsymbol{E}_h^{n-\frac{1}{2}})\right].$$

(III) Using (4.81) with n replaced by $n+1$ to subtract itself, we obtain

$$\epsilon_0(\delta_\tau^3\boldsymbol{E}_h^{n+\frac{1}{2}},\phi_h)=(\delta_\tau^2\boldsymbol{H}_h^{n+\frac{1}{2}},\nabla\times\phi_h)-(\delta_\tau^2\boldsymbol{J}_{d,h}^{n+\frac{1}{2}},\phi_h)-(\delta_\tau^2\overline{\boldsymbol{J}}_{p,h}^{n+\frac{1}{2}},\phi_h),\tag{4.85}$$

Using (4.82) to subtract itself with n reduced to $n-1$, we have

$$\mu_0(\delta_\tau^3\boldsymbol{H}_h^n,\psi_h)=-(\nabla\times\delta_\tau^2\boldsymbol{E}_h^n,\psi_h).\tag{4.86}$$

Using (4.83) to subtract itself with n replaced by $n-1$, we have

$$(\frac{1}{\epsilon_0\omega_{pe}^2}\delta_\tau^3\boldsymbol{J}_{d,h}^n+\frac{\gamma}{\epsilon_0\omega_{pe}^2}\delta_\tau^2\overline{\boldsymbol{J}}_{d,h}^n,\phi_h)=(\delta_\tau^2\boldsymbol{E}_h^n,\phi_h).\tag{4.87}$$

Choosing $\phi_h = \tau\delta_\tau^2\overline{\boldsymbol{E}}_h^{n+\frac{1}{2}}$, $\psi_h = \tau\delta_\tau^2\overline{\boldsymbol{H}}_h^n$, and $\phi_h = \tau\delta_\tau^2\overline{\boldsymbol{J}}_{d,h}^n$ in (4.85), (4.86), and (4.87), respectively, and summing up the results, we have

$$\begin{aligned}&\frac{\epsilon_0}{2}(\|\delta_\tau^2\boldsymbol{E}_h^{n+1}\|^2-\|\delta_\tau^2\boldsymbol{E}_h^{n}\|^2)+\frac{\mu_0}{2}(\|\delta_\tau^2\boldsymbol{H}_h^{n+\frac{1}{2}}\|^2-\|\delta_\tau^2\boldsymbol{H}_h^{n-\frac{1}{2}}\|^2)\\&\quad+\frac{1}{2\epsilon_0\omega_{pe}^2}(\|\delta_\tau^2\boldsymbol{J}_{d,h}^{n+\frac{1}{2}}\|^2-\|\delta_\tau^2\boldsymbol{J}_{d,h}^{n-\frac{1}{2}}\|^2)+\frac{\tau\gamma}{\epsilon_0\omega_{pe}^2}\|\delta_\tau^2\overline{\boldsymbol{J}}_{d,h}^{n}\|^2\\&=\frac{\tau}{2}\left[(\delta_\tau^2\boldsymbol{H}_h^{n+\frac{1}{2}},\nabla\times\delta_\tau^2\boldsymbol{E}_h^{n+1})-(\delta_\tau^2\boldsymbol{H}_h^{n-\frac{1}{2}},\nabla\times\delta_\tau^2\boldsymbol{E}_h^{n})\right]-\tau(\delta_\tau^2\overline{\boldsymbol{J}}_{p,h}^{n+\frac{1}{2}},\delta_\tau^2\overline{\boldsymbol{E}}_h^{n+\frac{1}{2}})\\&\quad+\frac{\tau}{2}\left[(\delta_\tau^2\boldsymbol{J}_{d,h}^{n-\frac{1}{2}},\delta_\tau^2\boldsymbol{E}_h^{n})-(\delta_\tau^2\boldsymbol{J}_{d,h}^{n+\frac{1}{2}},\delta_\tau^2\boldsymbol{E}_h^{n+1})\right],\end{aligned}\tag{4.88}$$

where we used the following identities

$$\begin{aligned}&(\delta_\tau^2\boldsymbol{H}_h^{n+\frac{1}{2}},\nabla\times\delta_\tau^2\overline{\boldsymbol{E}}_h^{n+\frac{1}{2}})-(\nabla\times\delta_\tau^2\boldsymbol{E}_h^n,\delta_\tau^2\overline{\boldsymbol{H}}_h^n)\\&=\frac{1}{2}\left[(\delta_\tau^2\boldsymbol{H}_h^{n+\frac{1}{2}},\nabla\times\delta_\tau^2\boldsymbol{E}_h^{n+1})-(\delta_\tau^2\boldsymbol{H}_h^{n-\frac{1}{2}},\nabla\times\delta_\tau^2\boldsymbol{E}_h^{n})\right]\end{aligned}$$

and

$$(\delta_\tau^2\overline{\boldsymbol{J}}_{d,h}^n,\delta_\tau^2\boldsymbol{E}_h^n)-(\delta_\tau^2\overline{\boldsymbol{E}}_h^{n+\frac{1}{2}},\delta_\tau^2\boldsymbol{J}_{d,h}^{n+\frac{1}{2}})=\frac{1}{2}\left[(\delta_\tau^2\boldsymbol{J}_{d,h}^{n-\frac{1}{2}},\delta_\tau^2\boldsymbol{E}_h^{n})-(\delta_\tau^2\boldsymbol{J}_{d,h}^{n+\frac{1}{2}},\delta_\tau^2\boldsymbol{E}_h^{n+1})\right].$$

(IV) Expanding (3.35) with n replaced by $n+1$ and multiplying the result by τ, we obtain

$$\begin{aligned}&\frac{1}{2}(\|\delta_\tau\boldsymbol{J}_{p,h}^{n+\frac{3}{2}}\|^2-\|\delta_\tau\boldsymbol{J}_{p,h}^{n+\frac{1}{2}}\|^2)+\tau b_1^*\|\delta_\tau\overline{\boldsymbol{J}}_{p,h}^{n+1}\|^2+\frac{b_2^*}{4}(\|\boldsymbol{J}_{p,h}^{n+2}\|^2-\|\boldsymbol{J}_{p,h}^{n}\|^2)\\&=\tau(a_2^*\delta_\tau^2\boldsymbol{E}^{n+1}+a_1^*\delta_{2\tau}\boldsymbol{E}^{n+1}+a_0^*\boldsymbol{E}^{n+1},\delta_\tau\overline{\boldsymbol{J}}_{p,h}^{n+1}).\end{aligned}\tag{4.89}$$

Adding up (4.80), (4.84), (4.88) and (4.89), and using the same identities given as step (V) in the proof of Theorem 2.1, we have

$$
\begin{aligned}
&\frac{\epsilon_0}{2}\left[(\|\boldsymbol{E}_h^{n+1}\|^2-\|\boldsymbol{E}_h^{n}\|^2)+(\|\delta_\tau\boldsymbol{E}_h^{n+\frac12}\|^2-\|\delta_\tau\boldsymbol{E}_h^{n-\frac12}\|^2)+(\|\delta_\tau^2\boldsymbol{E}_h^{n+1}\|^2-\|\delta_\tau^2\boldsymbol{E}_h^{n}\|^2)\right]\\
&\quad+\frac{\mu_0}{2}\left[(\|\boldsymbol{H}_h^{n+\frac12}\|^2-\|\boldsymbol{H}_h^{n-\frac12}\|^2)+(\|\delta_\tau\boldsymbol{H}_h^{n+1}\|^2-\|\delta_\tau\boldsymbol{H}_h^{n}\|^2)+(\|\delta_\tau^2\boldsymbol{H}_h^{n+\frac12}\|^2-\|\delta_\tau^2\boldsymbol{H}_h^{n-\frac12}\|^2)\right]\\
&\quad+\frac{1}{2\epsilon_0\omega_{pe}^2}\left[(\|\boldsymbol{J}_{d,h}^{n+\frac12}\|^2-\|\boldsymbol{J}_{d,h}^{n-\frac12}\|^2)+(\|\delta_\tau\boldsymbol{J}_{d,h}^{n+1}\|^2-\|\delta_\tau\boldsymbol{J}_{d,h}^{n}\|^2)+(\|\delta_\tau^2\boldsymbol{J}_{d,h}^{n+\frac12}\|^2-\|\delta_\tau^2\boldsymbol{J}_{d,h}^{n-\frac12}\|^2)\right]\\
&\quad+\frac{\tau\gamma}{\epsilon_0\omega_{pe}^2}(\|\overline{\boldsymbol{J}}_{d,h}^{n}\|^2+\|\delta_\tau\overline{\boldsymbol{J}}_{d,h}^{n+\frac12}\|^2+\|\delta_\tau^2\overline{\boldsymbol{J}}_{d,h}^{n}\|^2)\\
&\quad+\frac12(\|\delta_\tau\boldsymbol{J}_{p,h}^{n+\frac32}\|^2-\|\delta_\tau\boldsymbol{J}_{p,h}^{n+\frac12}\|^2)+\tau b_1^*\|\delta_\tau\overline{\boldsymbol{J}}_{p,h}^{n+1}\|^2+\frac{b_2^*}{4}(\|\boldsymbol{J}_{p,h}^{n+2}\|^2-\|\boldsymbol{J}_{p,h}^{n}\|^2)\\
&\quad+\tau a_2^*\|\delta_\tau^2\overline{\boldsymbol{E}}_h^{n+\frac12}\|^2+\frac{a_1^*}{2}(\|\delta_\tau\overline{\boldsymbol{E}}_h^{n+1}\|^2-\|\delta_\tau\overline{\boldsymbol{E}}_h^{n}\|^2)\\
&=\frac{\tau}{2}\left[(\boldsymbol{H}_h^{n+\frac12},\nabla\times\boldsymbol{E}_h^{n+1})-(\boldsymbol{H}_h^{n-\frac12},\nabla\times\boldsymbol{E}_h^{n})\right]-\tau(\overline{\boldsymbol{J}}_{p,h}^{n+\frac12},\overline{\boldsymbol{E}}_h^{n+\frac12})\\
&\quad-\frac{\tau}{2}\left[(\boldsymbol{J}_{d,h}^{n+\frac12},\boldsymbol{E}_h^{n+1})-(\boldsymbol{J}_{d,h}^{n-\frac12},\boldsymbol{E}_h^{n})\right]\\
&\quad+\frac{\tau}{2}\left[(\delta_\tau\boldsymbol{H}_h^{n},\nabla\times\delta_\tau\boldsymbol{E}_h^{n-\frac12})-(\delta_\tau\boldsymbol{H}_h^{n+1},\nabla\times\delta_\tau\boldsymbol{E}_h^{n+\frac12})\right]-\tau(\delta_\tau\overline{\boldsymbol{J}}_{p,h}^{n},\delta_\tau\overline{\boldsymbol{E}}_h^{n})\\
&\quad+\frac{\tau}{2}\left[(\delta_\tau\boldsymbol{J}_{d,h}^{n+1},\delta_\tau\boldsymbol{E}_h^{n+\frac12})-(\delta_\tau\boldsymbol{J}_{d,h}^{n},\delta_\tau\boldsymbol{E}_h^{n-\frac12})\right]\\
&\quad+\frac{\tau}{2}\left[(\delta_\tau^2\boldsymbol{H}_h^{n+\frac12},\nabla\times\delta_\tau^2\boldsymbol{E}_h^{n+1})-(\delta_\tau^2\boldsymbol{H}_h^{n-\frac12},\nabla\times\delta_\tau^2\boldsymbol{E}_h^{n})\right]\\
&\quad+\frac{\tau}{2}\left[(\delta_\tau^2\boldsymbol{J}_{d,h}^{n-\frac12},\delta_\tau^2\boldsymbol{E}_h^{n})-(\delta_\tau^2\boldsymbol{J}_{d,h}^{n+\frac12},\delta_\tau^2\boldsymbol{E}_h^{n+1})\right]\\
&\quad+\tau\left(\frac{b_1^*}{2}(\delta_\tau\overline{\boldsymbol{J}}_{p,h}^{n+1}+\delta_\tau\overline{\boldsymbol{J}}_{p,h}^{n})+b_2^*\overline{\overline{\boldsymbol{J}}}_{p,h}^{n+\frac12}-a_0^*\overline{\boldsymbol{E}}_h^{n+\frac12},\delta_\tau^2\overline{\boldsymbol{E}}_h^{n+\frac12}\right)\\
&\quad+\tau(a_2^*\delta_\tau^2\boldsymbol{E}_h^{n+1}+a_1^*\delta_\tau\overline{\boldsymbol{E}}_h^{n+1}+a_0^*\boldsymbol{E}_h^{n+1},\delta_\tau\overline{\boldsymbol{J}}_{p,h}^{n+1}).
\end{aligned}
\tag{4.90}
$$

(V) Now we just need to bound all the RHS terms in (4.90). Note that those RHS terms not in square brackets have been bounded in the proof of Theorem 3.2. Below we just need to bound those RHS terms in square brackets.

By using the inverse estimate (4.76) and the Cauchy–Schwarz inequality,we have

$$
\begin{aligned}
&\frac{\tau}{2}(\boldsymbol{H}_h^{n+\frac12},\nabla\times\boldsymbol{E}_h^{n+1})=\frac{\tau C_v}{2}(\sqrt{\mu_0}\boldsymbol{H}_h^{n+\frac12},\sqrt{\epsilon_0}\nabla\times\boldsymbol{E}_h^{n+1})\\
&\le\frac{\tau C_v C_{inv}h^{-1}}{2}\cdot\sqrt{\mu_0}\|\boldsymbol{H}_h^{n+\frac12}\|\cdot\sqrt{\epsilon_0}\|\boldsymbol{E}_h^{n+1}\|\\
&\le\frac{\tau C_v C_{inv}h^{-1}}{4}(\mu_0\|\boldsymbol{H}_h^{n+\frac12}\|^2+\epsilon_0\|\boldsymbol{E}_h^{n+1}\|^2).
\end{aligned}
\tag{4.91}
$$

By the Cauchy–Schwarz inequality, we easily have

$$
\begin{aligned}
&\frac{\tau}{2}(\boldsymbol{J}_{d,h}^{n+\frac12},\boldsymbol{E}_h^{n+1})=\frac{\tau\omega_{pe}}{2}(\frac{1}{\sqrt{\epsilon_0\omega_{pe}^2}}\boldsymbol{J}_{d,h}^{n+\frac12},\sqrt{\epsilon_0}\boldsymbol{E}_h^{n+1})\\
&\le\frac{\tau\omega_{pe}}{4}(\frac{1}{\epsilon_0\omega_{pe}^2}\|\boldsymbol{J}_{d,h}^{n+\frac12}\|^2+\epsilon_0\|\boldsymbol{E}_h^{n+1}\|^2).
\end{aligned}
\tag{4.92}
$$

By the same techniques, we have the following estimates for the rest terms:

$$\frac{\tau}{2}(\delta_\tau\boldsymbol{H}_h^{n+1},\nabla\times\delta_\tau\boldsymbol{E}_h^{n+\frac12})\le\frac{\tau C_v C_{inv}h^{-1}}{4}(\mu_0\|\delta_\tau\boldsymbol{H}_h^{n+1}\|^2+\epsilon_0\|\delta_\tau\boldsymbol{E}_h^{n+\frac12}\|^2),\tag{4.93}$$

$$\frac{\tau}{2}(\delta_\tau\boldsymbol{J}_{d,h}^{n+1},\delta_\tau\boldsymbol{E}_h^{n+\frac12})\le\frac{\tau\omega_{pe}}{4}(\frac{1}{\epsilon_0\omega_{pe}^2}\|\delta_\tau\boldsymbol{J}_{d,h}^{n+1}\|^2+\epsilon_0\|\delta_\tau\boldsymbol{E}_h^{n+\frac12}\|^2),\tag{4.94}$$

$$\frac{\tau}{2}(\delta_\tau^2\boldsymbol{H}_h^{n+\frac12},\nabla\times\delta_\tau^2\boldsymbol{E}_h^{n+1})\le\frac{\tau C_v C_{inv}h^{-1}}{4}(\mu_0\|\delta_\tau^2\boldsymbol{H}_h^{n+\frac12}\|^2+\epsilon_0\|\delta_\tau^2\boldsymbol{E}_h^{n+1}\|^2),\tag{4.95}$$

$$\frac{\tau}{2}(\delta_\tau^2 \boldsymbol{J}_{d,h}^{n+\frac{1}{2}}, \delta_\tau^2 \boldsymbol{E}_h^{n+1}) \le \frac{\tau\omega_{pe}}{4}(\frac{1}{\epsilon_0\omega_{pe}^2}\|\delta_\tau^2 \boldsymbol{J}_{d,h}^{n+\frac{1}{2}}\|^2 + \epsilon_0\|\delta_\tau^2 \boldsymbol{E}_h^{n+1}\|^2). \tag{4.96}$$

Summing up (4.90) from $n = 0$ to any $m > 0$, substituting the above estimates into the result, and using the time step constraint given by (3.41) and the following:

$$\frac{\tau C_v C_{inv} h^{-1}}{4} \le \frac{1}{8}, \quad \frac{\tau\omega_{pe}}{4} \le \frac{1}{8},$$

we conclude the proof by using the discrete Gronwall's inequality. □

Finally, we can prove the following optimal error estimate for our leap-frog scheme (4.70)–(4.73).

Theorem 4.2. *Under the same time step constraint as given in Theorem 4.1, we have the error estimate: For any $m \ge 0$,*

$$\begin{aligned}
&\epsilon_0(\|\boldsymbol{E}_h^{m+1} - \boldsymbol{E}(t_{m+1})\|^2 + \|\delta_\tau \boldsymbol{E}_h^{m+\frac{1}{2}} - \partial_t \boldsymbol{E}(t_{m+\frac{1}{2}})\|^2 + \|\delta_\tau^2 \boldsymbol{E}_h^{m+1} - \partial_{t^2}\boldsymbol{E}(t_{m+1})\|^2)\\
&+\mu_0(\|\boldsymbol{H}_h^{m+\frac{1}{2}} - \boldsymbol{H}(t_{m+\frac{1}{2}})\|^2 + \|\delta_\tau \boldsymbol{H}_h^{m+1} - \partial_t \boldsymbol{H}(t_{m+1})\|^2 + \|\delta_\tau^2 \boldsymbol{H}_h^{m+\frac{1}{2}} - \partial_{t^2}\boldsymbol{H}(t_{m+\frac{1}{2}})\|^2)\\
&+\frac{1}{\epsilon_0\omega_{pe}^2}(\|\boldsymbol{J}_{d,h}^{m+\frac{1}{2}} - \boldsymbol{J}_d(t_{m+\frac{1}{2}})\|^2 + \|\delta_\tau \boldsymbol{J}_{d,h}^{m+1} - \partial_t \boldsymbol{J}_d(t_{m+1})\|^2 + \|\delta_\tau^2 \boldsymbol{J}_{d,h}^{m+\frac{1}{2}} - \partial_{t^2}\boldsymbol{J}_d(t_{m+\frac{1}{2}})\|^2)\\
&+\|\delta_\tau \boldsymbol{J}_{p,h}^{m+\frac{3}{2}} - \partial_t \boldsymbol{J}_p(t_{m+\frac{3}{2}})\|^2 + a_1^*\|\delta_\tau \overline{\boldsymbol{E}}_h^{m+1} - \partial_t \overline{\boldsymbol{E}}(t_{m+1})\|^2\\
&+\frac{b_2^*}{2}(\|\boldsymbol{J}_{p,h}^{m+2} - \boldsymbol{J}_p(t_{m+2})\|^2 + \|\boldsymbol{J}_{p,h}^{m+1} - \boldsymbol{J}_p(t_{m+1})\|^2) \le C(h^p + \tau^2)^2,
\end{aligned} \tag{4.97}$$

where the positive constant C depends on the physical parameters ϵ_0, a_0^*, a_1^*, a_2^*, b_1^*, b_2, ω_{pe}, but is independent of h and τ.

Proof. Following the same technique developed in the proof of Theorem 3.3, we can obtain the E-error equation:

$$\begin{aligned}
&\epsilon_0(\delta_\tau \mathcal{E}_{h\xi}^{n+\frac{1}{2}}, \phi_h) - (\mathcal{H}_{h\xi}^{n+\frac{1}{2}}, \nabla\times\phi_h) + (\mathcal{J}_{d\xi}^{n+\frac{1}{2}} + \overline{\mathcal{J}}_{p\xi}^{n+\frac{1}{2}}, \phi_h)\\
&= \epsilon_0(\delta_\tau \mathcal{E}_{h\eta}^{n+\frac{1}{2}}, \phi_h) - (\mathcal{H}_{h\eta}^{n+\frac{1}{2}}, \nabla\times\phi_h) + (\mathcal{J}_{d\eta}^{n+\frac{1}{2}} + \overline{\mathcal{J}}_{p\eta}^{n+\frac{1}{2}}, \phi_h)\\
&\quad + \left(\boldsymbol{H}(t_{n+\frac{1}{2}}) - \frac{1}{\tau}\int_{t_n}^{t_{n+1}} \boldsymbol{H}(s)ds, \nabla\times\phi_h\right)\\
&\quad - \left(\boldsymbol{J}_d(t_{n+\frac{1}{2}}) + \bar{\boldsymbol{J}}_p(t_{n+\frac{1}{2}}) - \frac{1}{\tau}\int_{t_n}^{t_{n+1}} (\boldsymbol{J}_d(s) + \boldsymbol{J}_p(s))ds, \phi_h\right),
\end{aligned} \tag{4.98}$$

the H-error equation:

$$\begin{aligned}
&\mu_0(\delta_\tau \mathcal{H}_{h\xi}^n, \psi_h) + (\nabla\times\mathcal{E}_{h\xi}^n, \psi_h) = \mu_0(\delta_\tau \mathcal{H}_{h\eta}^n, \psi_h) + (\nabla\times\mathcal{E}_{h\eta}^n, \psi_h)\\
&\quad -(\nabla\times\boldsymbol{E}(t_n) - \frac{1}{\tau}\int_{t_{n-\frac{1}{2}}}^{t_{n+\frac{1}{2}}} \nabla\times\boldsymbol{E}(s)ds, \psi_h),
\end{aligned} \tag{4.99}$$

the J_d-error equation:

$$\begin{aligned}
&(\frac{1}{\epsilon_0\omega_{pe}^2}\delta_\tau \mathcal{J}_{d\xi}^n + \frac{\gamma}{\epsilon_0\omega_{pe}^2}\overline{\mathcal{J}}_{d\xi}^n - \mathcal{E}_{h\xi}^n, \phi_h) = (\frac{1}{\epsilon_0\omega_{pe}^2}\delta_\tau \mathcal{J}_{d\eta}^n + \frac{\gamma}{\epsilon_0\omega_{pe}^2}\overline{\mathcal{J}}_{d\eta}^n - \mathcal{E}_{h\eta}^n, \phi_h)\\
&\quad + \frac{\gamma}{\epsilon_0\omega_{pe}^2}(\frac{1}{\tau}\int_{t_{n-\frac{1}{2}}}^{t_{n+\frac{1}{2}}} \boldsymbol{J}_d(s)ds - \bar{\boldsymbol{J}}_d(t_n), \phi_h) + (\boldsymbol{E}(t_n) - \frac{1}{\tau}\int_{t_{n-\frac{1}{2}}}^{t_{n+\frac{1}{2}}} \boldsymbol{E}(s)ds, \phi_h),
\end{aligned} \tag{4.100}$$

and the J_p-error equation:

$$\begin{aligned}
&(\delta_\tau^2 \mathcal{J}_{p\xi}^n + b_1^*\delta_{2\tau}\mathcal{J}_{p\xi}^n + b_2^*\widetilde{\mathcal{J}}_{p\xi}^n - a_2^*\delta_\tau^2\mathcal{E}_{h\xi}^n - a_1^*\delta_{2\tau}\mathcal{E}_{h\xi}^n - a_0^*\mathcal{E}_{h\xi}^n, \phi_h)\\
&= (\delta_\tau^2 \mathcal{J}_{p\eta}^n + b_1^*\delta_{2\tau}\mathcal{J}_{p\eta}^n + b_2^*\widetilde{\mathcal{J}}_{p\eta}^n - a_2^*\delta_\tau^2\mathcal{E}_{h\eta}^n - a_1^*\delta_{2\tau}\mathcal{E}_{h\eta}^n - a_0^*\mathcal{E}_{h\eta}^n, \phi_h)\\
&\quad + \left([\delta_{2\tau}(\partial_t \boldsymbol{J}_p(t_n)) - \delta_\tau^2 \boldsymbol{J}_p(t_n)] + b_2^*[\frac{1}{2\tau}\int_{t_{n-1}}^{t_{n+1}} \boldsymbol{J}_p(s)ds - \widetilde{\boldsymbol{J}}_p(t_n)], \phi_h\right)\\
&\quad - \left(a_2^*[\delta_{2\tau}(\partial_t \boldsymbol{E}(t_n)) - \delta_\tau^2 \boldsymbol{E}(t_n)] + a_0^*[\frac{1}{2\tau}\int_{t_{n-1}}^{t_{n+1}} \boldsymbol{E}(s)ds - \boldsymbol{E}(t_n)], \phi_h\right).
\end{aligned} \tag{4.101}$$

Note that all LHS terms in the error Eqs. (4.98), (4.99), (4.100) and (4.101) have exactly the same form as the leapfrog scheme (4.70)–(4.73), while all RHS terms can be easily shown to be bounded by $O(h^p + \tau^2)$ in the L^2-norm.

Hence, following exactly the same techniques developed for proving the numerical stability in Theorem 4.1, we can obtain: For any $m \geq 0$,

$$\begin{aligned}
&\epsilon_0(\|\mathcal{E}_{h\xi}^{m+1}\|^2 + \|\delta_\tau \mathcal{E}_{h\xi}^{m+\frac{1}{2}}\|^2 + \|\delta_\tau^2 \mathcal{E}_{h\xi}^{m+1}\|^2) \\
&+ \mu_0(\|\mathcal{H}_{h\xi}^{m+\frac{1}{2}}\|^2 + \|\delta_\tau \mathcal{H}_{h\xi}^{m+1}\|^2 + \|\delta_\tau^2 \mathcal{H}_{h\xi}^{m+\frac{1}{2}}\|^2) \\
&+ \frac{1}{\epsilon_0 \omega_{pe}^2}(\|\mathcal{J}_{d\xi}^{m+\frac{1}{2}}\|^2 + \|\delta_\tau \mathcal{J}_{d\xi}^{m+1}\|^2 + \|\delta_\tau^2 \mathcal{J}_{d\xi}^{m+\frac{1}{2}}\|^2) + \|\delta_\tau \mathcal{J}_{p\xi}^{m+\frac{3}{2}}\|^2 \\
&+ a_1^*\|\delta_\tau \overline{\mathcal{E}}_{h\xi}^{m+1}\|^2 + \frac{b_2^*}{2}(\|\mathcal{J}_{p\xi}^{m+2}\|^2 + \|\mathcal{J}_{p\xi}^{m+1}\|^2) \leq C(h^p + \tau^2)^2, \qquad (4.102)
\end{aligned}$$

where we used the initial condition assumptions (4.74)–(4.75) and the same time step constraint given in Theorem 4.1.

Finally, using the triangle inequality, the estimate (4.102), the interpolation and projection error estimates (3.54)–(3.55), we conclude the proof. □

5. Numerical results

Note that the theoretical analysis holds true for both 2D and 3D problems just by interpreting the curl operators in 2D and 3D differently. For simplicity, here we present some 2D numerical results to verify our theoretical analysis for the concentrator model. Our test is carried out by using FEniCS [63] version 2016.1.0 installed under Ubuntu 14.04 on ThinkPad T440s Notebook (with 70 GHz CPU and 8 GB memory).

To test the convergence, we implement the leap-frog scheme (4.70)–(4.73). Since it is not easy to obtain the exact solution for the complicated graphene model (2.1)–(2.4), we first assume that the system has a solution for the electric field given as

$$\boldsymbol{E}(x,y,t) = \begin{pmatrix} E_x \\ E_y \end{pmatrix} = \begin{pmatrix} \cos(\omega\pi x)\sin(\omega\pi y) \\ -\sin(\omega\pi x)\cos(\omega\pi y) \end{pmatrix} e^{-\alpha t}. \qquad (5.103)$$

Then we integrate (2.2) to obtain a magnetic solution

$$\begin{aligned}
H(x,y,t) &= -\int^t \mu_0^{-1}\nabla\times \boldsymbol{E}dt = -\int^t \mu_0^{-1}(\partial_x E_y - \partial_y E_x)e^{-\alpha t}dt \\
&= -\frac{2\omega\pi}{\mu_0\alpha}e^{-\alpha t}\cos(\omega\pi x)\cos(\omega\pi y). \qquad (5.104)
\end{aligned}$$

Substituting (5.103) into (2.3) and integrating from 0 to t, we obtain

$$e^{\gamma t}\boldsymbol{J}_d(t) - \boldsymbol{J}_d(0) = \epsilon_0\omega_{pe}^2\int_0^t e^{\gamma t}\boldsymbol{E}dt = \epsilon_0\omega_{pe}^2\int_0^t e^{(\gamma-\alpha)t}\boldsymbol{E}dt \begin{pmatrix} \cos(\omega\pi x)\sin(\omega\pi y) \\ -\sin(\omega\pi x)\cos(\omega\pi y) \end{pmatrix},$$

which leads to an analytical $\boldsymbol{J}_d$ solution:

$$\boldsymbol{J}_d(x,y,t) = \begin{cases} \epsilon_0\omega_{pe}^2 t\boldsymbol{E}(x,y,t), & \text{if } \gamma = \alpha, \\ \frac{\epsilon_0\omega_{pe}^2}{\gamma-\alpha}(1-e^{(\alpha-\gamma)t})\boldsymbol{E}(x,y,t), & \text{if } \gamma \neq \alpha. \end{cases} \qquad (5.105)$$

To find an analytical solution $\boldsymbol{J}_p$ from (2.4), we solve the characteristic equation $\lambda^2 + b_1^*\lambda + b_2^* = 0$ to obtain

$$\lambda = \frac{-b_1^* \pm \sqrt{(b_1^*)^2 - 4b_2^*}}{2} = -\frac{b_1^*}{2} \pm \frac{i\Delta}{2}, \quad \text{where } \Delta = \sqrt{4b_2^* - (b_1^*)^2}, \qquad (5.106)$$

by considering that the practical data (2.5) yields $(b_1^*)^2 - 4b_2^* < 0$. It is easy to see that (2.4) has a particular solution $\boldsymbol{J}_p^*(x,y,t) = \frac{a_2^*\alpha^2 - a_1^*\alpha + a_0^*}{\alpha^2 - b_1^*\alpha + b_2^*}\boldsymbol{E}(x,y,t)$. Hence from (5.106), we can choose an analytical solution $\boldsymbol{J}_p$ given as:

$$\boldsymbol{J}_p(x,y,t) = \frac{a_2^*\alpha^2 - a_1^*\alpha + a_0^*}{\alpha^2 - b_1^*\alpha + b_2^*}\boldsymbol{E}(x,y,t) + e^{-\frac{b_1^* t}{2}}\left(\mathbf{c}_1\cos(\frac{t\Delta}{2}) + \mathbf{c}_2\sin(\frac{t\Delta}{2})\right), \qquad (5.107)$$

where $\mathbf{c}_1$ and $\mathbf{c}_2$ are two arbitrary linearly independent 2D vectors.

To accommodate the above exact solution, we have to a source term $\boldsymbol{f}$ to the original governing equation (2.1) such that

$$\boldsymbol{f}(x,y,t) = \epsilon_0\partial_t\boldsymbol{E} - \nabla\times H + \boldsymbol{J}_d + \boldsymbol{J}_p = -\left(\frac{2(\omega\pi)^2}{\mu_0\alpha} + \epsilon_0\alpha\right)\boldsymbol{E} + \boldsymbol{J}_d + \boldsymbol{J}_p. \qquad (5.108)$$

With this added source, we need to revise the first equation of the leap-frog scheme (4.70)–(4.73) as follows:

$$\epsilon_0(\delta_\tau \boldsymbol{E}_h^{n+\frac{1}{2}}, \phi_h) = (\boldsymbol{H}_h^{n+\frac{1}{2}}, \nabla\times\phi_h) - (\boldsymbol{J}_{d,h}^{n+\frac{1}{2}}, \phi_h) - (\overline{\boldsymbol{J}}_{p,h}^{n+\frac{1}{2}}, \phi_h) + (\boldsymbol{f}(t_{n+\frac{1}{2}}), \phi_h). \qquad (5.109)$$

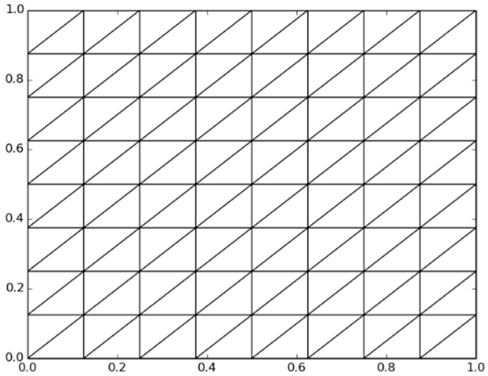

Fig. 2. A sample 8 × 8 mesh for our numerical test.

Note that our leap-frog scheme (5.109), (4.71)–(4.73) can be implemented as follows: At each time step,

Step 1. Solve for $\boldsymbol{H}_h^{n+\frac{1}{2}}$ from (4.71), and $\boldsymbol{J}_{d,h}^{n+\frac{1}{2}}$ from (4.72). Actually they can be done in parallel. Moreover, (4.72) can be simply updated as

$$\boldsymbol{J}_{d,h}^{n+\frac{1}{2}} = \frac{1-\frac{\tau\gamma}{2}}{1+\frac{\tau\gamma}{2}}\boldsymbol{J}_{d,h}^{n-\frac{1}{2}} + \frac{\tau\epsilon_0\omega_{pe}^2}{1+\frac{\tau\gamma}{2}}\boldsymbol{E}_h^n. \tag{5.110}$$

Step 2. From (4.73), we obtain

$$\begin{aligned}\boldsymbol{J}_{p,h}^{n+1} = &\frac{1}{1+\frac{\tau b_1^*}{2}+\frac{\tau^2}{2b_2}}\Big(2\boldsymbol{J}_{p,h}^n - (1-\frac{\tau b_1^*}{2}+\frac{\tau^2}{2b_2})\boldsymbol{J}_{p,h}^{n-1}\\ &+(a_2^*+\frac{\tau a_1^*}{2})\boldsymbol{E}_h^{n+1} + (\tau^2 a_0^* - 2a_2^*)\boldsymbol{E}_h^n + (a_2^* - \frac{\tau a_1^*}{2})\boldsymbol{E}_h^{n-1}\Big).\end{aligned} \tag{5.111}$$

Substituting (5.111) into (5.109) and reorganizing it, we have

$$\begin{aligned}&\left(\frac{\epsilon_0}{\tau}+\frac{a_2^*+\frac{\tau a_1^*}{2}}{2(1+\frac{\tau b_1^*}{2}+\frac{\tau^2}{2b_2})}\right)(\boldsymbol{E}_h^{n+1},\phi_h) = (\boldsymbol{H}_h^{n+\frac{1}{2}},\nabla\times\phi_h) - (\boldsymbol{J}_{d,h}^{n+\frac{1}{2}},\phi_h) + (\boldsymbol{f}(t_{n+\frac{1}{2}}),\phi_h)\\ &+\left(\frac{\epsilon_0}{\tau}-\frac{\tau^2 a_0^*-2a_2^*}{2(1+\frac{\tau b_1^*}{2}+\frac{\tau^2}{2b_2})}\right)(\boldsymbol{E}_h^n,\phi_h) - \frac{a_2^*-\frac{\tau a_1^*}{2}}{2(1+\frac{\tau b_1^*}{2}+\frac{\tau^2}{2b_2})}(\boldsymbol{E}_h^{n-1},\phi_h)\\ &-\left(\frac{1}{2}+\frac{1}{1+\frac{\tau b_1^*}{2}+\frac{\tau^2}{2b_2}}\right)(\boldsymbol{J}_{p,h}^n,\phi_h) + \frac{1-\frac{\tau b_1^*}{2}+\frac{\tau^2}{2b_2}}{2(1+\frac{\tau b_1^*}{2}+\frac{\tau^2}{2b_2})}(\boldsymbol{J}_{p,h}^{n-1},\phi_h).\end{aligned} \tag{5.112}$$

Hence, in **Step 2**, we first solve (5.112) for $\boldsymbol{E}_h^{n+1}$, then use (5.111) to update $\boldsymbol{J}_{p,h}^{n+1}$.

In our simulation, we simply choose the physical domain Ω as the unit square, which is partitioned by a structured triangular mesh. A sample coarse mesh is shown in Fig. 2. To test convergence rates, we use a sequence of uniformly refined meshes.

Example 1. First, we solved the case when $\alpha \neq \gamma$. For simplicity, we chose the physical parameters as follows:

$$\begin{aligned}&\epsilon_0 = \omega_{pe} = \alpha = b_1 = b_2 = a_0 = a_1 = a_2 = 1.0,\ \ \gamma = 0.1,\ \ \omega = 2,\\ &\mu_0 = 2\omega\pi/\alpha,\ \ \mathbf{c}_1 = \mathbf{c}_2 = \mathbf{0},\ \ T = 1e-6,\ \ \tau = 1e-9.\end{aligned}$$

The scheme (5.109), (4.71)–(4.73) is solved with the pth order Nédélec curl conforming edge element space $\boldsymbol{V}_h$ and the $(p-1)$th order L^2 finite element space U_h on triangular elements with $p = 1$ and $p = 2$. We solved this example on a series of uniformly refined $n \times n$ triangular meshes as Fig. 2. In Table 1, we presented the L^2 errors $\|\boldsymbol{E}_h^n - \boldsymbol{E}(t_n)\|$ and $\|\bar{H}_h^{n+\frac{1}{2}} - \bar{H}(t_{n+\frac{1}{2}})\|$ for the electric field $\boldsymbol{E}$ and the magnetic field H obtained at the last time step. Table 1 shows clearly the convergence rate of $O(h^p)$ in the L^2 norm for both $\boldsymbol{E}$ and H proved in Theorem 3.2. The corresponding CPU times (in seconds) are presented in Table 1 too. To illustrate the errors clearly, we also plot the solution errors versus $1/h$ in the log–log scale in Fig. 3 (Left), which shows $O(h^p)$ convergence for $p = 1$ and 2 clearly.

Table 1
Example 1: The L^2 errors obtained with pth order Nédélec curl conforming edge element for $\boldsymbol{E}$ and $(p-1)$th order L^2 basis function for H.

Meshes	$\boldsymbol{E}$ errors	Rates	H errors	Rates	CPU time (s)
			$p=1$		
4 × 4	3.175161E−01	–	2.515456E−01	–	9.13
8 × 8	1.599145E−01	0.9895	1.297322E−01	0.9553	12.74
16 × 16	8.010805E−02	0.9973	6.530812E−02	0.9902	17.34
32 × 32	4.007321E−02	0.9993	3.270732E−02	0.9976	33.55
64 × 64	2.003902E−02	0.9998	1.636025E−02	0.9994	113.86
128 × 128	1.001981E−02	0.9999	8.180949E−03	0.9999	478.38
			$p=2$		
Meshes	$\boldsymbol{E}$ errors	Rates	H errors	Rates	CPU time (s)
4 × 4	8.016165E−02	–	2.083166E−01	–	12.80
8 × 8	2.068098E−02	1.9546	6.003699E−02	1.7948	16.47
16 × 16	5.212563E−03	1.9882	1.555350E−02	1.9486	31.26
32 × 32	1.305838E−03	1.9970	3.923152E−03	1.9871	104.02
64 × 64	3.266844E−04	1.9990	9.829738E−04	1.9967	447.05
128 × 128	8.190780E−05	1.9958	2.458802E−04	1.9992	2345.66

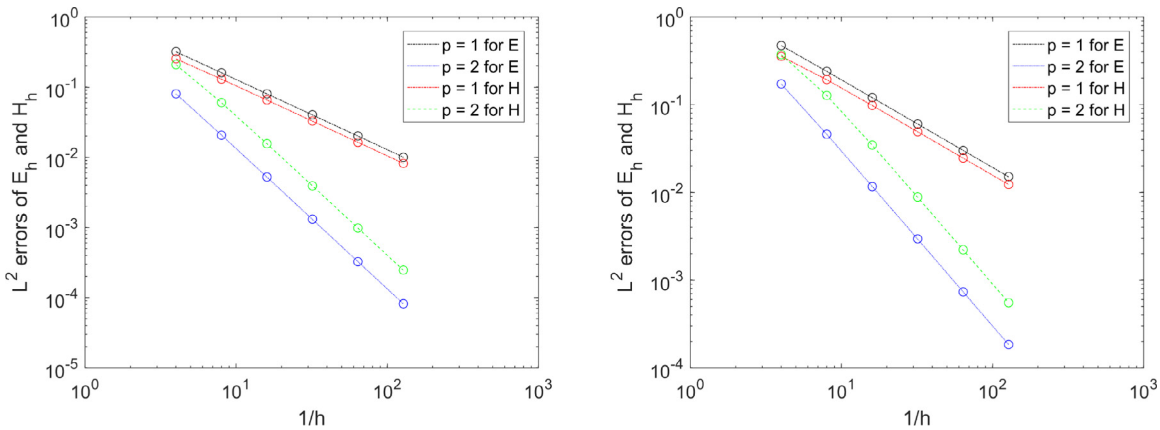

Fig. 3. Errors of $\|\boldsymbol{E}(t_N)-\boldsymbol{E}_h^N\|$ and $\|H(t_{N-\frac{1}{2}})-H_h^{N-\frac{1}{2}}\|$ versus $1/h$ in log–log scale for Example 1 (Left) and Example 2 (Right), respectively.

Example 2. In this example, we solved the case when $\alpha=\gamma$. More specifically, we used the following physical parameters:

$$\epsilon_0=\omega_{pe}=\alpha=\gamma=b_1=b_2=a_0=a_1=a_2=1.0,\ \omega=3,$$
$$\mu_0=2\omega\pi/\alpha,\ \boldsymbol{c}_1=(1,0)',\ \boldsymbol{c}_2=(0,1)',\ T=1e-6,\ \tau=1e-9.$$

The calculated L^2 errors for the electric field $\boldsymbol{E}$ and the magnetic field H obtained at the last time step are presented in Table 2, which clearly shows the convergence rate of $O(h^p)$ in the L^2 norm for both $\boldsymbol{E}$ and H again. The corresponding CPU times are presented in Table 2 too. Again, we also plot the solution errors versus $1/h$ in the log–log scale in Fig. 3 (Right), which shows $O(h^p)$ convergence for $p=1$ and 2 clearly for Example 2.

6. Conclusion

Compared to our previous work [60], we simplified the original governing equations for modeling wave propagation in graphene by eliminating two auxiliary unknowns and proposed two new finite element schemes which have the second order convergence in time, instead of only first order in time in [60]. A new stability for the revised modeling equations is established. Optimal error estimates and discrete stabilities for both schemes are proved. Interestingly, both discrete stabilities enjoy exactly the same form as the stability obtained in the continuous case. Considering that the Crank–Nicolson scheme's implementation is much more complicated and not that popular in practical simulations, we did not perform the convergence tests here. More numerical algorithms and interesting simulations will be explored in the future.

Table 2
Example 2: The L^2 errors obtained with pth order Nédélec curl conforming edge element for $\boldsymbol{E}$ and $(p-1)$th order L^2 basis function for H.

Meshes	$\boldsymbol{E}$ errors	Rates	H errors	Rates	CPU time (s)
			$p=1$		
4 × 4	4.703819E−01	–	3.546651E−01	–	11.34
8 × 8	2.391394E−01	0.9759	1.922349E−01	0.8835	12.48
16 × 16	1.200671E−01	0.9940	9.769043E−02	0.9765	18.02
32 × 32	6.009780E−02	0.9984	4.902784E−02	0.9946	34.50
64 × 64	3.005702E−02	0.9996	2.453627E−02	0.9986	110.37
128 × 128	1.502953E−02	0.9999	1.227091E−02	0.9996	465.86
			$p=2$		
4 × 4	1.717545E−01	–	3.712669E−01	–	13.01
8 × 8	4.591611E−02	1.9032	1.273013E−01	1.5442	16.41
16 × 16	1.168826E−02	1.9739	3.447982E−02	1.8844	32.10
32 × 32	2.935580E−03	1.9933	8.794404E−03	1.9710	104.82
64 × 64	7.348047E−04	1.9982	2.209641E−03	1.9927	440.28
128 × 128	1.839910E−04	1.9977	5.531023E−04	1.9982	2314.27

Declaration of competing interest

The authors declare that they have no known competing financial interests or personal relationships that could have appeared to influence the work reported in this paper.

Acknowledgments

The author is very grateful to two anonymous referees for their insightful comments on improving the paper.

References

[1] Novoselov KS, Geim AK, Morozov SV, Jiang D, Zhang Y, Dubonos SV, Grigorieva IV, Firsov AA. Electric field effect in atomically thin carbon films. Science 2004;306:666–9.
[2] Geim AK, Novoselov KS. The rise of graphene. Nature Mater 2007;6(3):183–91.
[3] Bonaccorso F, Sun Z, Hasan T, Ferrari AC. Graphene photonics and optoelectronics. Nature Photon 2010;4:611–22.
[4] Vakil A, Engheta N. Transformation optics using graphene. Science 2011;332(6035):1291–4.
[5] Bouzianas GD, Kantartzis NV, Antonopoulos CS, Tsiboukis TD. Optimal modeling of infinite graphene sheets via a class of generalized FDTD schemes. IEEE Trans Magn 2012;48(2):379–82.
[6] Nayyeri V, Soleimani M, Ramahi OM. Wideband modeling of graphene using the finite-difference time-domain method. IEEE Trans Antennas Prapagat 2013;61(12):6107–14.
[7] Mock A. Padé approximant spectral fit for FDTD simulation of graphene in the near infrared. Optic Mater Exp 2012;2(6):771–81.
[8] Hossain MdB, Rana MdM. An effective compact-FDTD wideband modeling of graphene conductuivity. In: 2015 international conference on electrical engineering and information communication technology. IEEE; 2015.
[9] Fisher A, Alvarez J, Gibson NL. Analysis of methods for the Maxwell-random Lorentz model. Result Appl Math 2020;8:100098.
[10] Hong J, Ji L, Kong L. Energy-dissipation splitting finite-difference time-domain method for Maxwell equations with perfectly matched layers. J Comput Phys 2014;269:201–14.
[11] Jenkinson MJ, Banks JW. High-order accurate FDTD schemes for dispersive Maxwell's equations in second-order form using recursive convolutions. J Comput Appl Math 2018;336:192–218.
[12] Li J, Chen M, Chen M. Developing and analyzing fourth-order difference methods for the metamaterial Maxwell's equations. Adv Comput Math 2019;45:213–41.
[13] Afshar F, Akbarzadeh-Sharbaf A, Giannacopoulos DD. A provably stable and simple FDTD formulation for electromagnetic modeling of graphene sheets. IEEE Trans Magn 2016;52(3):7203504.
[14] Karkkainen MK. Subcell FDTD modeling of electrically thin dispersive layers. IEEE Trans Microw Theory Tech 2003;51(6):1774–80.
[15] Zhang Y, Nguyen DD, Du K, Xu J, Zhao S. Time-domain numerical solutions of Maxwell interface problems with discontinuous electromagnetic waves. Adv Appl Math Mech 2016;8:353–85.
[16] Li W, Liang D, Lin Y. A new energy-conserved S-FDTD scheme for Maxwell's equations in metamaterials. Int J Numer Anal Model 2013;10:775–94.
[17] Lin H, Pantoja MF, Angulo LD, Alvarez J, Martin RG, Garcia SG. FDTD Modeling of graphene devices using complex conjugate dispersion material model. IEEE Microw Wirel Compon Lett 2012;22(12):612–4.
[18] Hao Y, Mittra R. FDTD modeling of metamaterials: theory and applications. Artech House Publishers; 2008.
[19] Taflove A, Hagness SC. Computational electrodynamics: The finite-difference time-domain method. 3rd ed.. Norwood, MA: Artech; 2005.
[20] Taflove A, Ardavan O, Steven GJ, editors. Advances in FDTD computational electrodynamics: photonics and nanotechnology. Norwood, MA: Artech; 2013.
[21] Bao G, Li P, Wu H. An adaptive edge element method with perfectly matched absorbing layers for wave scattering by biperiodic structures. Math Comp 2010;79:1–34.
[22] Boffi D, Costabel M, Dauge M, Demkowicz L, Hiptmair R. Discrete compactness for the p-version of discrete differential forms. SIAM J Numer Anal 2011;49:135–58.
[23] Bokil VA, Cheng Y, Jiang Y, Li F. Energy stable discontinuous Galerkin methods for Maxwell's equations in nonlinear optical media. J Comput Phys 2017;350:420–52.
[24] Bonito A, Guermond J-L, Luddens F. An interior penalty method with C0 finite elements for the approximation of the maxwell equations in heterogeneous media: convergence analysis with minimal regularity. ESAIM Math Model Numer Anal 2016;50(5):1457–89.

[25] Brenner SC, Gedicke J, Sung L-Y. Hodge decomposition for two-dimensional time harmonic Maxwell's equations: impedance boundary condition. Math Methods Appl Sci 2017;40:370–90.
[26] Buffa A, Houston P, Perugia I. Discontinuous Galerkin computation of the Maxwell eigenvalues on simplicial meshes. J Comput Appl Math 2007;204:317–33.
[27] Cao L, Zhang Y, Allegretto W, Lin Y. Multiscale asymptotic method for Maxwell's equations in composite materials. SIAM J Numer Anal 2010;47:4257–89.
[28] Carstensen C, Demkowicz L, Gopalakrishnan J. Breaking spaces and forms for the DPG method and applications including Maxwell equations. Comput Math Appl 2016;72(3):494–522.
[29] Chung ET, Ciarlet Jr P. A staggered discontinuous Galerkin method for wave propagation in media with dielectrics and meta-materials. J Comput Appl Math 2013;239:189–207.
[30] Duan H, Liu W, Ma J, Tan RCE, Zhang S. A family of optimal Lagrange elements for Maxwell's equations. J Comput Appl Math 2019;358:241–65.
[31] Hoppe RHW, Yousept I. Adaptive edge element approximation of H(curl)-elliptic optimal control problems with control constraints. BIT 2015;55:255–77.
[32] Li J, Huang Y, Yang W, Wood A. Mathematical analysis and time-domain finite element simulation of carpet cloak. SIAM J Appl Math 2014;74(4):1136–51.
[33] Li J, Shi C, Shu C-W. Optimal non-dissipative discontinuous Galerkin methods for Maxwell's equations in Drude metamaterials. Comput Math Appl 2017;73:1768–80.
[34] Li J, Hesthaven J. Analysis and application of the nodal discontinuous Galerkin method for wave propagation in metamaterials. J Comput Phys 2014;258:915–30.
[35] Scheid C, Lanteri S. Convergence of a discontinuous Galerkin scheme for the mixed time domain Maxwell's equations in dispersive media. IMA J Numer Anal 2013;33(2):432–59.
[36] Sun M, Li J, Wang P, Zhang Z. Superconvergence analysis of high-order rectangular edge elements for time-harmonic Maxwell's equations. J Sci Comput 2018;75(1):510–35.
[37] Zhong L, Chen L, Shu S, Wittum G, Xu J. Quasi-optimal convergence of adaptive edge finite element methods for three dimensional indefinite time-harmonic Maxwell's equations, Math Comp 81 (278) 623–642.
[38] Chung ET, Du Q, Zou J. Convergence analysis of a finite volume method for Maxwell's equations in nonhomogeneous media. SIAM J Numer Anal 2003;41:37–63.
[39] Huang Y, Li J, Yang W. Modeling backward wave propagation in metamaterials by the finite element time domain method. SIAM J Sci Comput 2013;35:B248–74.
[40] Xie Z, Wang J, Wang B, Chen C. Solving maxwell's equation in meta-materials by a CG-DG method. Commun Comput Phys 2016;19(5):1242–64.
[41] Tsantili IC, Cho MH, Cai W, Karniadakis GE. A computational stochastic methodology for the design of random meta-materials under geometric constraints. SIAM J Sci Comput 2018;40:B353–78.
[42] Yao C, Lin Y, Wang C, Kou Y. A third order linearized BDF scheme for Maxwell's equations with nonlinear conductivity using finite element method. Int J Numer Anal Model 2017;14:511–31.
[43] Nicaise S, Scheid C. Stability and asymptotic properties of a linearized hydrodynamic medium model for dispersive media in nanophotonics. Comput Math Appl 2020;79:3462–94.
[44] Tsuji P, Engquist B, Ying L. A sweeping preconditioner for time-harmonic Maxwell's equations with finite elements. J Comput Phys 2012;231(9):3770–83.
[45] Yang Z, Wang L-L, Rong Z, Wang B, Zhang B. Seamless integration of global Dirichlet-to-Neumann boundary condition and spectral elements for transformation electromagnetics. Comput Methods Appl Mech Engrg 2016;301:137–63.
[46] Ciarlet Jr P, Zou J. Fully discrete finite element approaches for time-dependent Maxwell's equations. Numer Math 1999;82:193–219.
[47] Chen Z, Du Q, Zou J. Finite element methods with matching and nonmatching meshes for Maxwell's equations with discontinuous coefficients. SIAM J Numer Anal 2000;37:1542–70.
[48] Ciarlet Jr P, Wu H, Zou J. Edge element methods for Maxwell's equations with strong convergence for Gauss' laws. SIAM J Numer Anal 2014;52:779–807.
[49] Anees A, Angermann L. Time domain finite element method for Maxwell's equations. IEEE Access 2019;7:63852–67.
[50] Hiptmair R. Finite elements in computational electromagnetism. Acta Numer 2002;11:237–339.
[51] Cassier M, Joly P, Kachanovska M. Mathematical models for dispersive electromagnetic waves: An overview. Comput Math Appl 2017;74(11):2792–830.
[52] Teixeira FL. Time-domain finite-difference and finite-element methods for Maxwell equations in complex media. IEEE Trans Antennas Propag 2008;56(8):2150–66.
[53] Demkowicz L, Kurtz J, Pardo D, Paszynski M, Rachowicz W, Zdunek A. Computing with hp-adaptive finite elements. 2: Frontiers: Three dimensional elliptic and maxwell problems with applications. CRC Press, Taylor and Francis; 2008.
[54] Hesthaven JS, Warburton T. Nodal discontinuous Galerkin methods: Algorithms, analysis, and applications. New York: Springer; 2008.
[55] Monk P. Finite element methods for Maxwell's equations. Oxford: Oxford University Press; 2003.
[56] Li J, Huang Y. Time-domain finite element methods for Maxwell'S equations in metamaterials. Springer ser. comput. math., vol. 43, New York: Springer; 2013.
[57] Rodriguez AA, Valli A. Eddy Current approximation of maxwell equations: theory, algorithms and applications. Springer; 2010.
[58] Maier M, Margetis D, Luskin M. Dipole excitation of surface plasmon on a conducting sheet: finite element approximation and validation. J Comput Phys 2017;339:126–45.
[59] Song JH, Maier M, Luskin M. Adaptive finite element simulations of waveguide configurations involving parallel 2D material sheets. Comput Methods Appl Mech Engrg 2019;351:20–34.
[60] Yang W, Li J, Huang Y. Time-domain finite element method and analysis for modeling of surface plasmon polaritons. Comput Methods Appl Mech Engrg 2020;372:113349.
[61] Evans LC. Partial differential equations. American Mathematical Society; 1998.
[62] Quarteroni A, Valli A. Numerical approximation of partial differential equations. Springer ser. comput. math., vol. 23, Berlin: Springer; 1994.
[63] Logg A, Mardal K-A, Wells GN, editors. Automated solution of differential equations by the finite element method: The FEniCS book. Springer; 2012.